Supplementary Materials to

ZAP-70 Catalytic Activity Regulates Basal Signaling and Negative Feedback of the Proximal TCR Signaling Pathway

Hanna Sjölin Goodfellow[1,2##], *Maria P. Frushicheva*[*3], *Qinqin Ji*[*4], *Debra A Cheng*[1,2], *Aaron J. Cantor*[5,6], *John Kuriyan*[5-9], *Arup K. Chakraborty*[*3,10-14#], *Arthur Salomon*[*4,15-16#], *Arthur Weiss*[*1,2#]

One Sentence Summary: ZAP-70 negatively regulates basal and induced TCR signaling.

[1]Howard Hughes Medical Institute, UCSF, San Francisco, California, USA, 94143

[2]Department of Medicine, UCSF, San Francisco, California, USA, 94143

[3]Department of Chemical Engineering, Massachusetts Institute of Technology, Cambridge, Massachusetts, USA, 02142

[4]Department of Chemistry, Brown University, Providence, Rhode Island, USA, 02912

[5]Department of Molecular and Cell Biology, University of California, Berkeley, CA 94720, USA

[6]California Institute for Quantitative Biosciences, University of California, Berkeley, CA 94720, USA

[7]Department of Chemistry, University of California, Berkeley, CA 94720, USA

[8]Howard Hughes Medical Institute, University of California, Berkeley, CA 94720, USA

[9]Physical Biosciences Division, Lawrence Berkeley National Laboratory, Berkeley, CA 94720, USA

Departments of [10]Physics, [11]Chemistry, & [12]Biological Engineering, [13]Institute of Medical Engineering & Science, Massachusetts Institute of Technology, Cambridge, Massachusetts, USA, 02142

[14]Ragon Institute of MGH, MIT, & Harvard, Cambridge, Massachusetts, USA, 02139

Departments of [4]Chemistry, [15]Molecular Biology, Cell Biology, and Biochemistry, [16]Molecular Pharmacology, Physiology, and Biotechnology, Brown University, Providence, Rhode Island, USA, 02912

Running Title: ZAP-70-mediated negative regulation of TCR signaling

** contributed equally*

To whom correspondence should be addressed: as@brown.edu, arupc@mit.edu, aweiss@medicine.ucsf.edu

Present Address: Department of Experimental Medical Science, Section for Immunology, Lund University, Lund, Sweden

1. Experimental Procedures

1.1 Protein reduction, alkylation, digestion and peptide immunoprecipitation

Cell lysates from ZAP-70AS cells treated with (heavy SILAC label) and without (light SILAC label) inhibitor were combined with equal cell equivalents and reduced with 10 mM DTT for 20 minutes at 60°C, followed by alkylation with 100 mM iodoacetamide for 15 minutes at room temperature (RT) in the dark. Cell lysates were then diluted 4-fold with 20 mM HEPES buffer, pH 8.0 and digested with sequencing grade modified trypsin (Worthington, Lakewood, NJ) at a 1:1 (w/w) trypsin: protein ratio overnight at RT. Tryptic peptides were acidified to pH 2.0 by adding 1/20 volume of 20% trifluoroacetic acid (TFA) for a final concentration of 1% TFA, cleared at 1800 × g for 5 minutes at RT, and desalted using C18 Sep-Pak plus cartridges (Waters, Milford, MA) as described (*1*), with the exception that TFA was used instead of acetic acid at the same required concentrations. Eluents containing peptides were lyophilized for 48 hours to dryness.

Peptide immunoprecipitation was performed using p-Tyr-100 phosphotyrosine antibody beads (Cell Signaling Technology). Dry peptides from each time point were reconstituted in ice-cold immunoaffinity purification (IAP) buffer (5 mM MOPS pH 7.2, 10 mM sodium phosphate, 50 mM NaCl) and further dissolved through gentle shaking for 30 minutes at RT and brief

sonication in a sonicator water bath. Prior to peptide immunoprecipitation, a 10 pmol fraction of synthetic phosphopeptide LIEDAEpYTAK was added to each time point sample as an exogenous quantitation standard. Peptide solutions were then cleared at 1800 × g for 5 minutes at RT, combined with p-Tyr-100 phosphotyrosine antibody beads, and incubated for 2 hours at 4 °C. Beads were then washed three times with IAP buffer and twice with cold ddH_2O, and eluted with 0.15% TFA. Eluted peptides were then desalted using C18 Zip Tip pipette tips (Millipore Corporation Billerica, MA) as described (*2*).

1.2 Automated nano-LC/MS

LC/MS was performed as described previously (*1*). Tryptic peptides were analyzed by a fully automated phosphoproteomic technology platform (*3*, *4*). Phosphopeptides were eluted into a Linear Trap Quadropole (LTQ)/Orbitrap Velos mass spectrometer (Thermo Fisher Scientific, Waltham, MA) through a PicoFrit analytical column (360 μm outer diameter 75 μm inner diameter-fused silica with 15 cm of 3-μm Monitor C18 particles; New Objective, Woburn, MA) with a reversed phase gradient (0-70% 0.1M acetic acid in acetonitrile in 60 minutes, with a 90 min total method duration). An electrospray voltage of 1.8 kV was applied using a split flow configuration, as described previously (*5*). Spectra were collected in positive ion mode and in cycles of one full MS scan in the Orbitrap (m/z: 300-1700), followed by data-dependent MS/MS scans in the LTQ (~ 0.3 seconds each), sequentially of the ten most abundant ions in each MS scan with charge state screening for +1, +2, +3 ions and dynamic exclusion time of 30 seconds. The automatic gain control was 1,000,000 for the Orbitrap scan and 10,000 for the LTQ scans. The maximum ion time was 100 milliseconds for the LTQ scan and 500 milliseconds for the Orbitrap full scan. Orbitrap resolution was set at 60,000.

1.3 Data analysis

MS/MS spectra were searched against the non-redundant human UniProt complete proteome set database containing 72,078 forward and an equal number of reversed decoy protein entries using the Mascot algorithm provided with Matrix Science (*6*). Peak lists were generated using extract_msn.exe 07/12/07 using a mass range of 600-4500. The Mascot database search was performed with the following parameters: trypsin enzyme cleavage specificity, 2 possible missed cleavages, 7 ppm mass tolerance for precursor ions, 0.5 Da mass tolerance for fragment ions.

Search parameters specified a dynamic modification of phosphorylation (+79.9663 Da) on serine, threonine, and tyrosine residues, and methionine oxidation (+15.9949 Da), and a static modification of carbamidomethylation (+57.0215 Da) on cysteine. Search parameters also include a differential modification for arginine (+10.00827 Da) and lysine (+8.01420 Da) amino acids for the SILAC labeling. To provide high confidence phosphopeptide sequence assignments, data was filtered for Mowse score (>20 for all charge states) for Mascot results. In addition, a logistic spectral score (*7*) filter was applied to achieve a final estimated decoy database estimated false discovery rate (FDR) of <1%. FDR was estimated with the decoy database approach after final assembly of non-redundant data into heatmaps (*8*). To validate the position of the phosphorylation sites, the Ascore algorithm (*9*) was applied to all data, and the reported phosphorylation site position reflected the top Ascore prediction.

1.4 Quantitation of Relative Phosphopeptide Abundance

Relative quantitation of phosphopeptide abundance was performed via calculation of select ion chromatogram (SIC) peak areas for heavy and light SILAC-labeled phosphopeptides. For label-free comparison of phosphopeptide abundance in ZAP-70^{AS} cells treated without inhibitor among different time points of TCR stimulation, individual SIC peak areas were normalized to an exogeneously spiked standard phosphopeptide LIEDAEpYTAK peak area. The LIEDAEpYTAK phosphopeptide was added in the same amount to every LC/MS sample and accompanied cellular phosphopeptides through the peptide immunoprecipitation, desalt, and reversed-phase elution into the mass spectrometer. Peak areas were calculated by inspection of SICs using software programmed in Microsoft Visual Basic 6.0 based on Xcalibur Development kit 2.1 (Thermo Fisher Scientific). Quantitative data was calculated automatically for every assigned phosphopeptide using the ICIS algorithm available in the Xcalibur XDK. A minimum SIC peak area equivalent to the typical spectral noise level of 10000 was required of all data reported for label-free quantitation.

A label-free data heatmap was generated for comparison of phosphopeptides through a time course of receptor stimulation as previously described (*1*). The magnitude of change of the heatmap color was calculated through the natural log of the ratio of the fold change of each individual phosphopeptide peak area compared with the geometric mean for that phosphopeptide across all time points as described previously (*1*). In the heatmap representation, the geometric

mean of a given phosphopeptide across all time points was set to the color black. A blue color represented below average abundance, while yellow represented above average abundance for each unique phosphopeptide. Blanks in the heatmap indicated that a clearly defined SIC peak was not observed for that phosphopeptide in any of the replicate analyses for that time point. The heatmap colors were generated from the average of the LIEDAEpYTAK standard phosphopeptide normalized SICs in the five replicate experiments. The coefficient of variation (CV) was calculated for each heatmap square. Label free *p* values were calculated from the replicate data for each time point compared to the time point with the minimum average peak area for that phosphopeptide. *Q* values for multiple hypothesis tests were also calculated for each time point based on the determined *p* values using the R package QVALUE as previously described (*10*, *11*). A white dot on a label free heatmap square indicated that a significant difference (Q value < 5%) was detected for that phosphopeptide and timepoint relative to the timepoint with the minimal value.

In the second type of heatmap, SILAC ratios corresponding to phosphopeptide abundance differences between ZAP-70AS cells treated with and without inhibitor across the time course of receptor stimulation were represented (Table S1 and S2). For the SILAC heatmap, a black color represented a ratio of 1 between inhibitor treated and control samples for the peak area of a given phosphopeptide at that time point. A red color represented less abundance, and green represented higher abundance of the given phosphopeptide in ZAP-70AS cells treated with inhibitor compared ZAP-70AS cells treated without inhibitor. The magnitude of change of the heatmap color was calculated as described (*1*). *Q* values were also calculated based on replicate measurements for each phosphopeptide and time point (Table S3). A white dot on a SILAC heatmap square indicated that a significant change (Q value < 5%) was observed between the replicate data from the ZAP-70AS treated with and without inhibitor samples for that time point and phosphopeptide.

1.5 Reproducibility of SILAC experimental data

Pairwise comparisons of phosphopeptide peak areas from individual samples were generated. In order to limit the effect of a few phosphopeptides with a large ratio, log2 transformed peak areas were used for these comparisons. There are 5 replicates per time point for SILAC light and heavy samples, 160 nonredundant sample pairs could be constructed; Fig. S1

shows a subset of this data for 20 plots corresponding to all 0 min sample pairs. Pearson's correlation coefficient (*R)* indicated the degree of reproducibility. In order to provide a visualization of similarity of individual samples for all 160 pairs, the dots from 80 pairwise comparison plots for heavy samples were shown in one plot (Fig. S2A), and pearson's correlation coefficient was recalculated to indicate the reproducibility. The reproducibility of light samples was evaluated in the same way (Fig. S2B).

Fig. S1. Pairwise comparisons of Log2 transformed peak area for time point1.

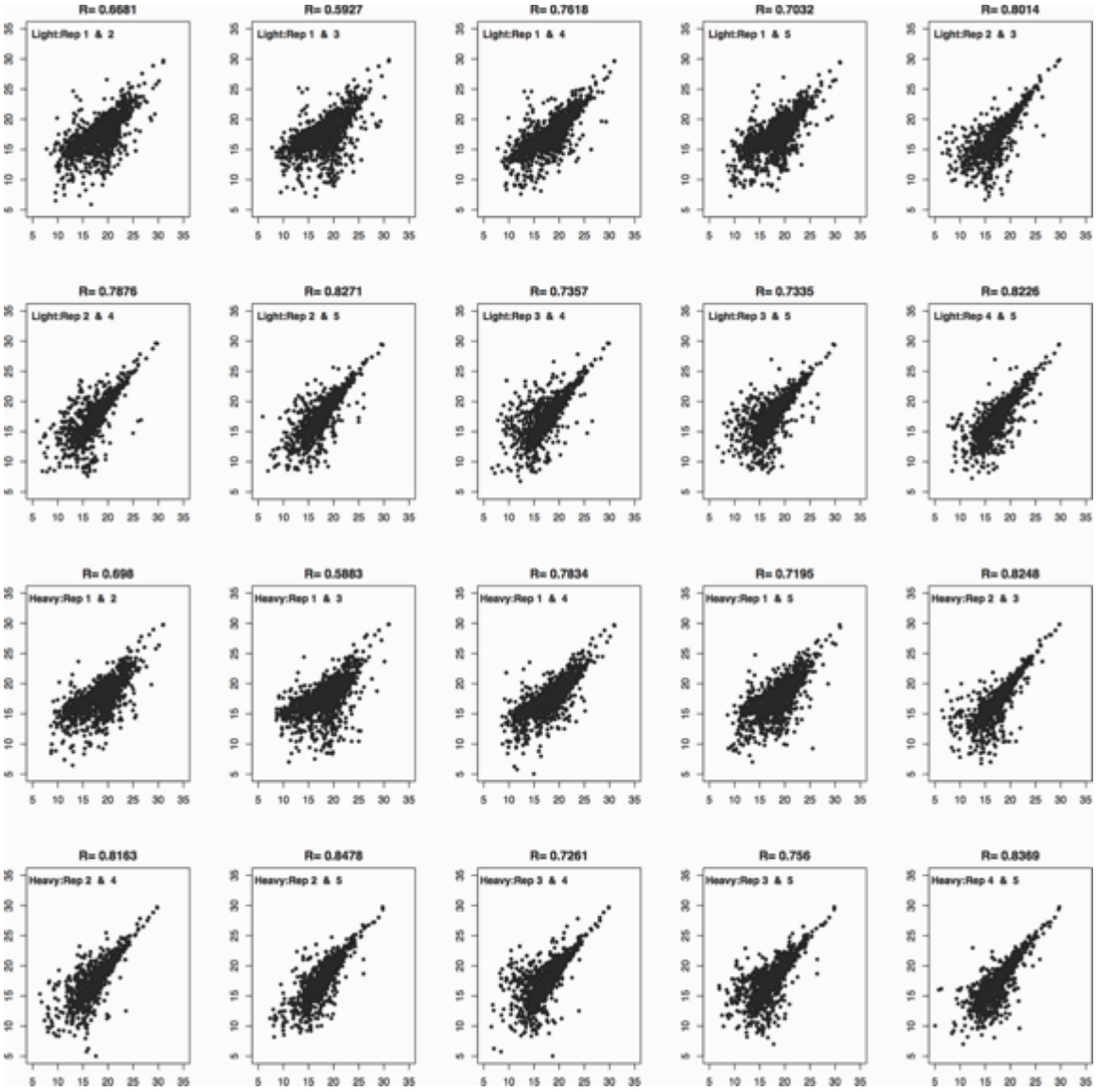

Fig. S2. Pairwise comparisons for all time points. **(A)** Pairwise comparisons for Log2 transformed peak area for SILAC heavy samples. **(B)** Pairwise comparisons for Log2 transformed peak area for SILAC light samples. (**C**) Pairwise comparisons of Log2 transformed SILAC ratios for all samples.

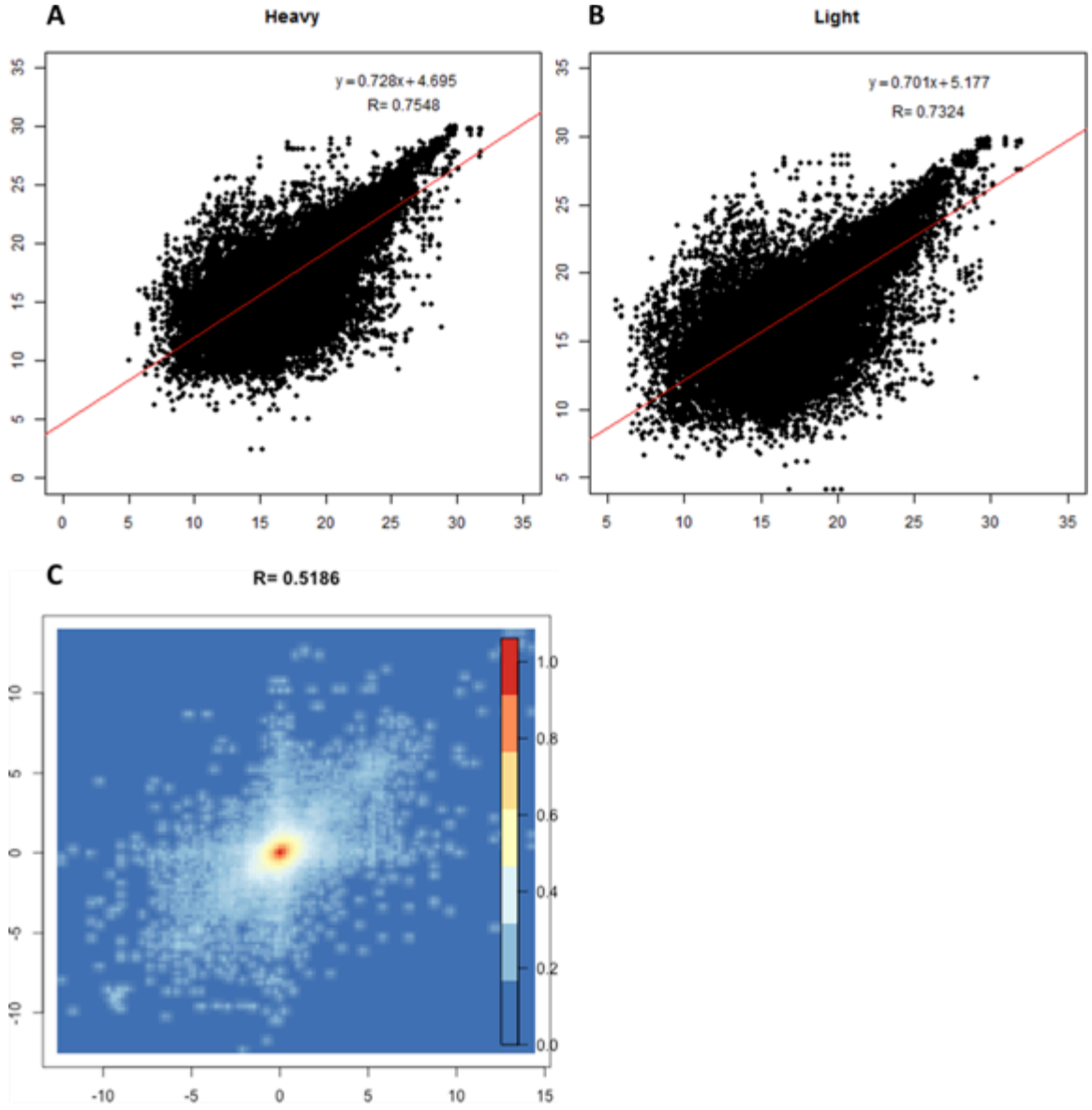

Table S1. Complete list of sequence and phosphorylation site assignments of all identified phosphopeptides with corresponding SIC peak areas and statistics, protein accession numbers, gene ontology and KEGG functional annotation. Included in this table are confident MSMS peptide assignment at >20 MOWSE score, <2 ppm mass error and logistic

score filter to achieve a final estimated 1% FDR by decoy database approach. Only forward database hits are included in this table.

Table S2. Complete list of phosphopeptides detected from every replicate and time point of TCR stimulation. Included in these tables are all phosphotyrosine containing peptides with MOWSE score >20 and mass error <2 ppm including decoy database reversed sequence hits. Reserved hits, if any for each replicate and time point are labeled with protein descriptor ###REV### and a 'R' designation in database direction. Listed are the assigned names of the corresponding proteins, the position of the phosphorylation site within the protein sequences, and the assigned peptide sequence. For the peptide sequence, * represents phosphorylation, and # represents Met oxidation. Every reported peptide includes the Logistic Spectral Validation score and Mascot Mowse score reflecting confidence in the sequence assignment and the Ascore, which reports the confidence in the localization of the phosphorylation site. Also reported is the mass error in ppm, the isolated mass of the peptide, the charge state, and the scan number

Table S3. Fold change and Q value for peptides listed in Table 1 of main text.

		0 min		2 min		5 min		10 min	
rotein Name	**phosphosite annotated**	**Fold change**	***Q* value**	**Fold change**	***Q* value**	**Fold change**	***Q* value**	**Fold change**	***Q* value**
ATP6V1E	Y56	1.2	0.294	2.3	0.068	**1.6**	**0.031**	1.3	0.224
CblB	Y665	2.6	0.356	-3.2	0.051	**-2.5**	**0.043**	1.2	0.490
CD28	Y191*	1.1	0.442	**-1.4**	**0.049**	-1.2	0.124	-1.2	0.256
CD28	Y206Y209*	**-2.1**	**0.036**	-1.7	0.190	1.6	0.469	-1.4	0.109
CD3E	Y199*	1.0	0.488	**1.2**	**0.039**	1.2	0.056	1.5	0.139
CD3 ζ	Y64Y72*	1.2		-2.7	0.071	**-2.3**	**0.038**	-1.5	0.172
CD3 ζ	Y72*	1.3	0.350	1.2	0.104	2.0	0.161	**1.7**	**0.028**
CD3 ζ	Y83*	1.1	0.269	1.3	0.105	**1.2**	**0.023**	1.4	0.070
CD3 ζ	Y111*	1.1	0.317	**1.3**	**0.037**	**1.2**	**0.030**	1.5	0.095
CD3 ζ	Y123*	1.2		1.6	0.176	1.3	0.499	1.7	0.119
CD3 ζ	Y142*	1.1	0.349	**1.2**	**0.048**	2.1	0.277	2.0	0.349
CD3 ζ	Y142*	1.0	0.489	1.2	0.071	1.1	0.105	1.4	0.167

CD3 ζ	Y142*	1.0	0.489	1.2	0.071	1.1	0.105	1.4	0.167
CD3 ζ	Y153*	**-1.5**	**0.046**	-2.0	0.074	1.0	0.510	1.9	0.264
CD3 δ	Y149Y160*	1.2	0.219	**1.5**	**0.016**	**1.5**	**0.030**	1.8	0.090
CD3 δ	Y149*	1.2	0.141	1.3	0.069	**1.4**	**0.044**	**1.8**	**0.020**
CD3 δ	Y149S161*	1.1	0.364	**1.6**	**0.035**	**1.5**	**0.016**	1.9	0.092
CD3 δ	Y160*	-1.0	0.460	**1.2**	**0.045**	1.2	0.054	1.5	0.105
ERK1	T202Y204*	-2.7		-2.7	0.248	-7.0		**-12.3**	**0.027**
ERK1	Y204*	-8.5		**-7.1**	**0.044**	-5.1	0.153	-7.5	0.069
ERK2	T185Y187*	-3.3		**-13.1**	**0.034**	-7.9	0.167	**-8.3**	**0.044**
ERK2	T185Y187*	-3.3		**-13.1**	**0.034**	-7.9	0.167	**-8.3**	**0.044**
ERK2	Y187*	1.6	0.280	**-4.7**	**0.038**	-4.5	0.114	**-5.4**	**0.033**
ERK2	Y187*	1.6	0.280	**-4.7**	**0.038**	-4.4	0.050	**-5.4**	**0.033**
GSK3B	Y71	-1.0	0.447	-1.3	0.241	**-2.7**	**0.012**	-2.5	0.101
ITK	Y146	-2.3	0.155	**-10.6**	**0.046**	-1.6	0.288	-2.7	0.073
ITK	Y512*	-1.2	0.297	**-2.0**	**0.028**	-1.4	0.054	-1.2	0.241
Lck	Y192*	**-8.3**	**0.001**	**-6.9**	**0.011**	**-7.3**	**0.007**	**-7.0**	**0.005**
Lck	Y394*	1.3	0.500	1.1	0.440	1.3	0.168	**1.6**	**0.040**
Lck	Y470	1.0	0.501	9.3	0.130	**7.6**	**0.013**	1.1	0.146
MAPK14	T180Y182*	1.4	0.104	**-3.4**	**0.044**	-2.6	0.169		
NCK1	Y105*	**-70.7**	**0.022**	-2.8	0.141	-4.0	0.209	-4.5	0.135
PI3K regulatory α	Y467*	1.1	0.052	1.2		1.2	0.071	**1.2**	**0.033**
PI3K regulatory γ	Y199	-1.7	0.097	-1.4	0.174	**-1.5**	**0.023**	-1.4	0.116
RXR-alpha	Y150	-1.6		-1.6	0.224	-1.2	0.286	**-1.3**	**0.036**
PLCγ1	Y771*	-1.1	0.388	**-2.4**	**0.031**	**-1.8**	**0.044**	-1.6	0.122
SHP-1	S556Y564*	1.5	0.306	-2.8	0.071	-2.5	0.079	**-2.4**	**0.045**
SHP-2	Y62*	**-1.3**	**0.007**	-1.3	0.173	-1.6	0.203	-1.2	0.060
PYK2	Y579*	**7.4**	**0.027**	**35.3**	**0.017**	**35.0**	**0.001**	**36.3**	**0.012**
PYK2	Y579Y580*	1.2	0.486	1.7	0.331	1.5	0.248	**2.4**	**0.043**

PYK2	Y580*	**23.6**	**0.036**	8.5	0.051	13.4	0.105	21.2	0.071
Tec	Y519	1.2	0.519	**-2.2**	**0.023**	-1.3	0.156	-1.2	0.270
VAV1	Y791	-1.2	0.288	**-3.0**	**0.017**	-1.8	0.105	-1.7	0.069
VAV3	Y265	1.5	0.380	-1.7	0.255	**-2.6**	**0.028**	-1.7	0.169
ZAP70	T286Y292*	-1.5	0.168	**-7.2**	**0.023**	**-6.6**	**0.032**	**-4.9**	**0.033**
ZAP70	S289Y292*	-1.5	0.168	**-7.2**	**0.023**	**-6.6**	**0.032**	**-4.9**	**0.033**
ZAP70	Y292*	-1.0	0.467	**-1.5**	**0.037**	**-1.6**	**0.044**	1.1	0.509
ZAP70	S301Y319	1.2	0.368	**1.1**	**0.045**	-1.0	0.446	1.6	0.295
ZAP70	Y315Y319	1.2	0.361	**1.1**	**0.045**	1.0	0.513	23.6	0.295
ZAP70	S491Y493*	-1.0	0.430	**2.0**	**0.001**	**1.7**	**0.012**	2.2	0.116
ZAP70	Y492Y493*	-1.0	0.470	**2.0**	**0.001**	**1.8**	**0.019**	2.4	0.125
ZAP70	Y493*	1.1	0.461	**2.6**	**0.022**	**2.2**	**0.040**	2.4	0.080
ZAP70	Y597Y598	1.0	0.522	-1.8	0.064	**-2.6**	**0.030**	-1.6	0.147
ZAP70	Y597	-1.1	0.363	-1.4	0.195	**-1.9**	**0.044**	-1.4	0.140
ZAP70	Y597Y598	1.3	0.305	-1.6	0.080	**-2.4**	**0.045**	-1.5	0.199
ZAP70	Y597S599	1.3	0.305	-1.6	0.080	**-2.4**	**0.045**	-1.5	0.199
ZAP70	Y598	1.2	0.068	-1.1	0.139	**-1.4**	**0.045**	-1.2	0.267

1.6 Cell stimulation and lysate preparation for Western blot validation of inhibitor specificity and SILAC data results.

P116 cells reconstituted with WT or AS2 ZAP-70 were resuspended at 10^8 cells/ml Dulbecco's PBS with Ca^+Mg^+ and allowed to rest at 37 C for 30 minutes. Ninety seconds prior to stimulation, cells were treated with 10μM HXJ42 or vehicle. OKT3 and OKT4 antibodies were added to cells to a final concentration of 0.25μg/ml, and thirty seconds later the antibodies were crosslinked with Goat anti-mouse IgG at a final concentration of 22μg/ml. At the indicated time points, the cells were pelleted and lysed in ice cold 1% NP40 lysis buffer containing protease and phosphatase inhibitors. Lysates were centrifuged at 4 C for 15 minutes at 16000 x

G. Lysates were then transferred into tubes containing an equal volume of 2X SDS sample buffer containing 2-mercaaptoethanol. Lysates were run on SDS-PAGE gels, transferred to Immobilon membranes and Western blots were performed. Data are representative of at least three independent experiments (Fig. S3).

Antibodies: OKT3, OKT4 (eBiosciences); LAT-pY132 (Invitrogen/BIOSOURCE); ZAP70-pY319, ZAP-70-pY493, p44/42 MAPK pThr202/Tyr204 (Cell Signalling); Lck (1F6 from J. B. Bolen); pY (4G10; Upstate Biotechnology); LAT (Abcam); ERK1/2, Slp76 (Santa Cruz); CD3ζ-pY142 (BD Pharmagin); pY 128 SLP76 (BD Biosciences); Goat α-Rabbit IgG (H+L)-HRP and Goat α-Mouse IgG (H+L)-HRP (Southern Biotech). The following antibodies have been described previously: 2F3.2 (ZAP70) and 6B10.2 (CD3ζ).

Fig. S3. Inhibitor Specificity Validation. **(A)** HXK42 inhibits ZAP70-dependent signaling in ZAP70-deficient p116 cells expressing the AS2-ZAP70 mutant but not cells expressing WT ZAP70. Whole cell lysates from WT- or AS2-ZAP70 reconstituted P116 cells were stimulated by anti-CD3 and anti-CD4 crosslinking in the presence or absence of 10mM HXJ42 for the indicated time points. Lysates were immunoblotted for the total tyrosine phosphorylated proteins, as well and phospho-specific sites of Erk, LAT, Slp76, ZAP-70, and CD3-ζ (zeta) chain. Data are representative of at least three independent experiments. **(B)** HXJ42 inhibits basal phosphorylation of some proteins. Phosphorylated proteins were quantified and normalized to expression of total protein using Image Lab 5.2 software (Bio-Rad), from three separate experiments.

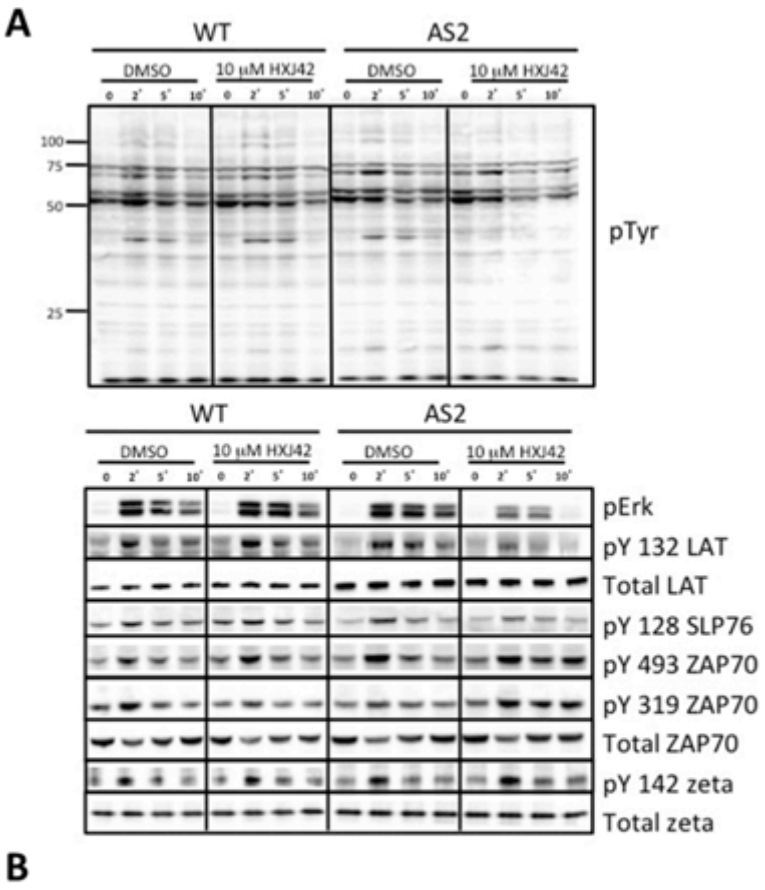

B

Phosphorylation site	Mean basal fold increase with HXJ42	Standard deviation
ZAP70 pY493	1.45	.12
Zeta pY142	1.42	.22
Lck pY394	1.29	.30

1.7 Measurements of Lck-SH2 binding affinities to the singly phosphorylated ITAMs

The Lck SH2 domain (residues 126–223) was expressed in *E. coli* with an N-terminal hexahistidine + protein G tag. It was purified using a nickel affinity capture step, followed by tag removal using TEV protease, a subtractive nickel affinity step, and size exclusion chromatography. The concentration of the Lck SH2 was determined spectrophotometrically using the method of Edelhoch (*12*), with a calculated extinction coefficient of 9530 M^{-1} cm^{-1} at

280 nm wavelength. The singly phosphorylated ITAM peptides, corresponding to residues 69–87 of human TCR ζ, were synthesized by ELIM Biopharmeceuticals (Hayward, CA). Peptide concentrations were determined spectrophotometrically at 205 nm wavelength with an extinction coefficient of 66,500 M^{-1} cm^{-1}, as calculated using the method of Anthis and Clore (*13*). Isothermal titration calorimetry was performed using an auto-ITC_{200} instrument from GE (Piscataway, NJ) at 25°C. Prior to experiments, the protein and peptides were dialyzed for ≥24 hours against binding buffer containing 25 mM HEPES, 150 mM NaCl, 1 mM TCEP, pH 7.5, with two changes of buffer. The Lck SH2 was used as the syringe titrant, and the peptide was used as the cell reactant. After an initial injection of 0.5 µl, 19 injections of 2 µl of Lck SH2 into peptide were recorded. Fitting was performed in the Origin software provided by the instrument manufacturer with a one-set-of-sites model after subtracting a constant value of from the integrated heats to correct for the heat of dilution. The reported binding parameters are from a single representative experiment (Fig. S4 and Table S4).

Fig. S4. Binding of the SH2 domain of Lck to monophosphorylated TCR ζ-chain ITAM peptides. Isothermal titration calorimetry was used to determine the binding affinity of the isolated SH2 domain of human Lck (residues 126–223) to monophosphorylated peptides corresponding to the N-terminal ITAM of human TCR ζ (residues 69–87, numbering including the signal peptide). The peptides were phosphorylated on either the N-terminal tyrosine **(A)** or the C-terminal tyrosine **(B)**. Binding thermograms (top) and isotherms with fits from a one-set-of-sites binding model (bottom) for representative experiments at 25°C are shown. The heat of the first injection for both runs and that of the twelfth injection from C-terminally phosphorylated peptide run were omitted from the fitting. A constant value of 0.75 kcal mol^{-1}, chosen based on the goodness of fit, was subtracted from the integrated heats in both runs to bring the baseline heat of dilution to zero. The Lck SH2 domain was the syringe titrant, at 359 µM, and the peptide was the cell reactant, at 30 µM. The apparent binding parameters from fits to the data for these individual runs is presented in Table S4. Deviation of the stoichiometry parameter *n* from a value of 1 reflects inaccuracy in the measured peptide concentration. The fitted values of the association constant and molar enthalpy change upon binding do not depend on *n*.

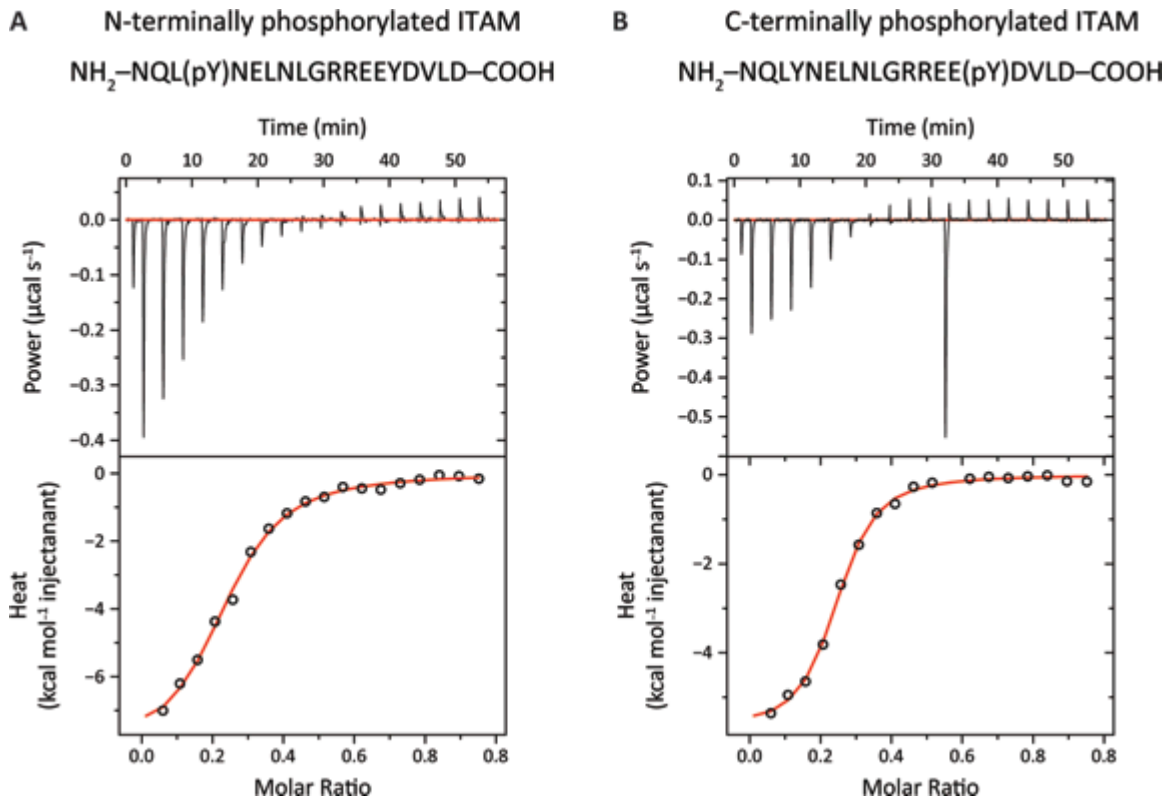

Table S4. Binding parameters for the Lck SH2 domain and monophosphorylated ζ ITAM peptides determined by ITC at 25°C.[a]

peptide sequence	n[b]	K_A (M^{-1})	K_D (µM)	ΔH^o (cal mol^{-1})	$T\Delta S^o$ (cal mol^{-1})
NQL(pY)NELNLGRREEYDVLD	0.596 ± 0.013[c]	$3.82\times10^5 \pm 4.0\times10^4$	2.6 ± 0.3	−8259 ± 244	−644
NQLYNELNLGRREE(pY)DVLD	0.59 ± 0.007	$9.75\times10^5 \pm 9.6\times10^4$	1.0 ± 0.1	−5745 ± 95	2426

[a] All reported parameters are apparent values obtained by fitting a one-set-of-sites binding model to the results of a single representative ITC experiment. n, stoichiometry; K_A, association constant; K_D, dissociation constant; ΔH^o, molar enthalpy of binding; $T\Delta S^o$, molar entropy of binding × 298 K.

[b] Deviation from the value of 1 for the stoichiometry parameter is primarily a result of inaccurately measured peptide concentrations.

[c] Uncertainty is standard error of the mean from the non-linear least squares fitting

2. Computational Modeling

2.1 Plasma-membrane Environment Affects Lck-SH2 Kinetics

The experimental ZAP-70 null / ZAP-70 reconstituted SILAC ratio shows an asymmetry in phosphorylation of N- and C- terminal tyrosine residues in each ζ-chain ITAM (Fig. 5A of main text). To reproduce this asymmetry we used the observations found in B cells (*14*). Specifically, the Src family kinase binds with its SH2 domain to singly phosphorylated ITAMs. Once bound, the Src kinase increases its catalytic activity and rapidly phosphorylates the neighboring site of ITAM. We applied these B cell observations to our calculations in T cells using the Src family kinase, Lck. The calculated SILAC ratios using these effects ("ITAM & Lck" model, shown in Fig. 5A of main text) require that Lck-SH2 binds to the singly phosphorylated ITAMs with high affinity (comparable to ZAP-70 binding affinity to the doubly phosphorylated ITAMs). Once bound, Lck rapidly phosphorylates the neighboring terminal tyrosine residues within each ζ-chain ITAM (with faster kinetics than initial ITAM phosphorylation), creating the doubly phosphorylated ITAMs. These faster kinetic effects may emerge from the effect of the membrane environment, because Lck is located, by virtue of its myristoylation and palmitoylation, in the plasma-membrane, whereas ZAP-70 has no lipid modification and is in the cytoplasm. The membrane environment results in increased protein concentrations and correlations in 2-dimensions that result in enhanced rebinding events. This may result in a higher fraction of bound enzyme-substrate pairs (*15*, *16*). To test this assumption, we roughly estimated the number of the rebinding events of Lck-SH2 to the singly phosphorylated ITAMs.

The number of enzyme-substrate rebinding events was calculated using Bell's model (*17*) for the membrane (2D case) and the cytoplasm (3D case) environments. The total dwell time t_a over the duration of all rebinding events is (*18*):

$$t_a = t_{1/2} + \frac{1}{K_D} \cdot \left[\frac{\ln(2)}{k_{on}^*} \right] \tag{S1}$$

$$k_{on}^* = 2\pi(D_E + D_s) \tag{S2}$$

where k_{on}^{*} is a threshold k_{on} above which rebindings are relevant, the D_E and D_s are the diffusion constants of enzyme and substrate, respectively. In general, whenever k_{on} exceeds this threshold, at least one rebinding is expected to occur. In the membrane environment, the threshold k_{on}^{*} value equals 60,000 $\mu m^2/s$ and in the cytoplasm it is $5 \cdot 10^8$ $\mu m^2/s$ (taken from (*17*, *18*)). The half-time $t_{1/2}$ accounts for the duration of the first binding event, whereas the second term of Eq.S1 accounts for any subsequent rebinding events. Since the duration of every individual binding events lasts, on average, as long as any other, the expected number of rebinding events between enzyme-substrate is (*18*):

$$\bar{N} = \frac{t_a}{t_{1/2}} - 1 = \frac{k_{on}}{k_{on}^{*}} \tag{S3}$$

Depending on the k_{on} and k_{on}^{*} values (here we associate it with the substrate binding affinity K_D and the diffusion coefficient, respectively), the system has qualitatively different behavior (shown in Fig. S5). When k_{on} rates are high (high binding affinity) many rebinding events occur between enzyme and substrate, reaching quasiequilibrium before diffusing away. However, when k_{on} rates are low (low binding affinity) the rebinding events occur very rarely. Additionally, upon moving from the cytoplasm to the membrane environment (via decreasing the diffusion coefficient (or the threshold value k_{on}^{*})) the number of rebinding events increases.

Furthermore, Fig. S5 also provides a good correlation with the experimentally measured binding affinities of Lck-SH2 to the singly and ZAP-70 to the doubly phosphorylated ITAMs (*19*). The top left corner of Fig. S5 represents a low number of rebindings events of ZAP-70 to the singly phosphorylated ITAMs, which is consistent with its low binding affinity (5 μM (*19*)). ZAP-70 binds strongly to the doubly phosphorylated ITAMs (k_D ~ 5 nM (*19*, *20*). Therefore, the number of the rebindings increases (as illustrated at the top right corner of Fig. S5). The measured binding affinity of Lck-SH2 to the singly phosphorylated ITAM in solution is low (1 μM (*19*)), and thus one would expect a low number of rebinding events. However, we assumed that Lck is in the membrane environment, and therefore the number of rebindings is high (shown at the bottom right corner of Fig. S5). Therefore, the Lck-SH2 binding affinity to the singly phosphorylated ITAM could potentially be comparable to the binding affinity of the ZAP-70 to the doubly phosphorylated ITAMs. However, this assumption requires further experimental

measurements of the Lck-SH2 binding affinity to the singly phosphorylated ITAMs in the membrane environment.

Fig. S5. An estimated number of enzyme-substrate rebinding events upon moving from the membrane (2D case) to the cytoplasm (3D case) environment with increasing substrate binding affinity (K_D).

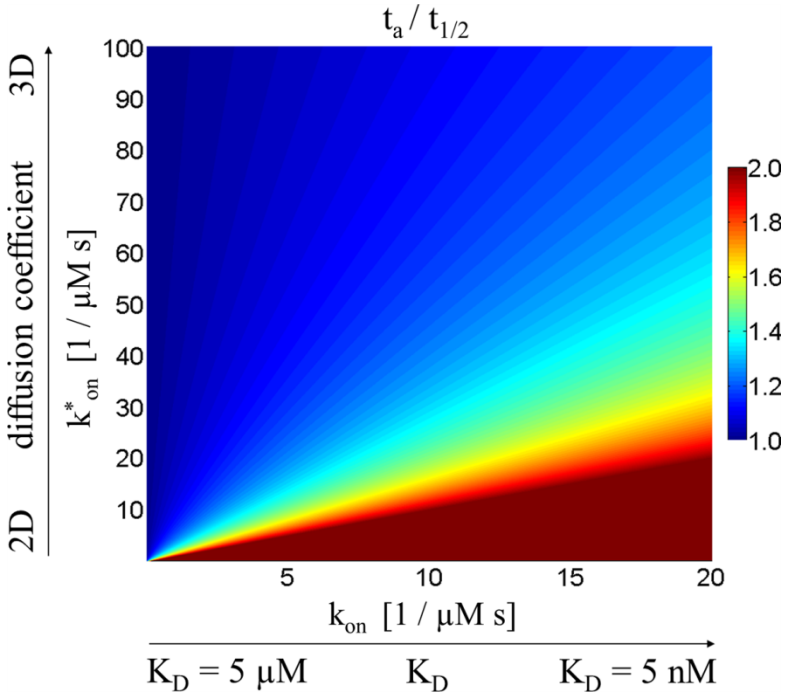

2.2 Estimate of High Lck Effective Concentration

To reproduce the ITAM asymmetrical phosphorylation of ZAP-70 null / ZAP-70 reconstituted SILAC ratio (Fig. 5A of main text), we found that Lck-SH2 binds strongly to the singly phosphorylated ITAMs. Once bound, Lck rapidly phosphorylates the neighboring terminal tyrosine residues within each ζ-chain ITAM (with faster kinetics than initial ITAM phosphorylation). This is because the strongly bound Lck has a higher effective concentration for phosphorylation of the neighboring tyrosine. Namely, once Lck binds to singly phosphorylated ITAMs, its high effective concentration promotes a faster phosphorylation of the adjacent ITAM site.

Using Michaelis-Menten kinetics, we estimated Lck effective concentration that is localized to the singly and doubly phosphorylated ITAMs and compared it to the amount of ZAP-70 bound to the doubly phosphorylated ITAMs.

$$E + S \leftrightarrow E{:}S \tag{S4}$$

$$K_D = [E][S] / [ES] \tag{S5}$$

$$[E] + [ES] = [E]_0 \tag{S6}$$

where E enzyme, S substrate, E:S enzyme-substrate complex, K_D is a dissociation constant, [E] is concentration of free enzyme, [ES] is concentration of bound enzyme, $[E]_0$ is total enzyme concentration. Lck and ZAP-70 are enzymes and the singly and doubly phosphorylated ITAMs are substrates.

Substituting Eq.S6 to Eq. S5, we obtained

$$K_D = ([E]_0 - [ES])\,[S] / [ES] = ([E]_0 / [ES] - 1)\,[S] \tag{S7}$$

If we assume that $K_D >> [S]$, leading to

$$K_D \approx [E]_0 / [ES] \tag{S8}$$

then the concentration of bound enzyme is

$$[ES] = [E]_0 / K_D \tag{S9}$$

Using Eq.S9 and experimentally measured binding affinities, we calculated the effective concentrations of Lck and ZAP-70 bound to the singly and doubly phosphorylated ITAMs.

First, we calculated the concentration of Lck bound to the singly phosphorylated ITAMs.

$$Lck(A,SH2) + ITAM(N_p,C_0) \leftrightarrow Lck(A,SH2){:}ITAM(N_p,C_0) \tag{S10}$$

$$K_{D1}^{Lck} = [Lck(A,SH2)][ITAM(N_p,C_0)] / [Lck(A,SH2){:}ITAM(N_p,C_0)] \tag{S11}$$

Substituting Eq.S9 to Eq.S11, we obtained:

$$[Lck(A,SH2){:}ITAM(N_p,C_0)] = [Lck(A,SH2)][ITAM(N_p,C_0)] / K_{D1}^{Lck} \approx [Lck(A)]_0 / K_{D1}^{Lck} \tag{S12}$$

If total concentration of Lck $[Lck(A)]_0$ = 1.67 μM (estimated from our calculations) and $K_{D1}^{Lck,exp}$ = 5 μM (*19*), then the concentration of bound Lck to the singly phosphorylated ITAMs $[Lck(A,SH2):ITAM(N_p,C_0)]$ = 0.334 μM.

Once Lck bound with its SH2 non-catalytic domain to the singly phosphorylated ITAMs, it rapidly binds with its catalytic domain to the neighboring terminal tyrosine residues within each ITAM and promotes the subsequent phosphorylation events.

$$Lck(A,SH2):ITAM(N_p,C_0) \leftrightarrow Lck(A,SH2):ITAM(N_p,C_0):Csite \quad (S13)$$

$$K_{D2}^{Lck} = [Lck(A,SH2):ITAM(N_p,C_0)]/ [Lck(A,SH2):ITAM(N_p,C_0):Csite] \quad (S14)$$

Therefore, the amount of Lck bound to ITAMs:

$$[Lck(A,SH2):ITAM(N_p,C_0):Csite] = [Lck(A,SH2)][ITAM(N_p,C_0)] / K_{D1}^{Lck} \cdot K_{D2}^{Lck} \quad (S15)$$

Substituting Eq.S9 to Eq.S15, we obtained:

$$[Lck(A,SH2):ITAM(N_p,C_0):Csite] \approx [Lck(A)]_0 / K_{D1}^{Lck} \cdot K_{D2}^{Lck} \quad (S16)$$

If K_{D2}^{Lck} = 5 μM (estimated from the threshold that ZAP-70 binds more strongly to the doubly phosphorylated ITAMs than Lck ($K_D^{ZAP-70,exp} > K_{D1}^{Lck,exp} \cdot K_{D2}^{Lck}$)), then the concentration of bound Lck to ITAMs $[Lck(A,SH2):ITAM(N_p,C_0):Csite]$ = 66800 μM.

Next, we calculated the amount of ZAP-70 to the doubly phosphorylated ITAMs.

$$ZAP\text{-}70 + ITAM(N_p,C_p) \leftrightarrow ZAP\text{-}70:ITAM(N_p,C_p) \quad (S17)$$

$$K_D^{ZAP-70} = [ZAP\text{-}70][ITAM(N_p,C_p)] / [ZAP\text{-}70:ITAM(N_p,C_p)] \quad (S18)$$

Substituting Eq.S9 to Eq.S18, we obtained:

$$[ZAP\text{-}70:ITAM(N_p,C_p)] = [ZAP\text{-}70][ITAM(N_p,C_p)] / K_D^{ZAP-70} \approx [ZAP\text{-}70]_0 / K_D^{ZAP-70}$$

If total concentration of ZAP-70 $[ZAP\text{-}70]_0$ = 0.83 μM (estimated from our calculations) and $K_D^{ZAP-70,exp}$ = 5 nM (*19*), then the concentration of ZAP-70 bound to the doubly phosphorylated ITAMs $[ZAP\text{-}70:ITAM(N_p,C_p)]$ = 166 μM.

These estimates provide support for the increased kinetic effects considered in our computational model. The amount of ZAP-70 bound to the doubly phosphorylated ITAMs is greater than the amount of Lck bound to the singly phosphorylated ITAMs, which is in the agreement with the experimentally measured Lck and ZAP-70 binding affinities (*19*). In addition, our estimates show that once the Lck binds with its SH2 domain to the singly phosphorylated ITAMs, its effective concentration increases and further promotes subsequent phosphorylation events. This is similar to B cell observations (*14*).

2.3 Additional Computational Model: Including ZAP-70 allosteric function

A recent study of ITAM-ζ1 peptide-binding affinities to ZAP-70 (*20*) suggests another mode of ZAP-70 regulation. Deindl *et al.* (*20*) show that the ZAP-70 WT in its open conformation binds to the ITAM-ζ1 peptide with high affinity (K_D=76.7 nM). The mutations of Y315F and Y319F in the SH2-linker domain of ZAP-70, which stabilize its autoinhibited conformation, slightly reduces the ITAM peptide-binding affinity (K_D=96.1 nM). This difference in the binding affinities suggests the possibility of ZAP-70 allosteric regulation having an impact on ITAM binding, where the inhibitor in the ZAP-70^{AS}+Inhibitor cells might influence ZAP-70 conformation along with its kinase activity. To explore the consequences of this allosteric regulation of ZAP-70, we incorporated this effect in our model (shown in Fig. S6).

The model for the ZAP-70-reconstituted and ZAP-70^{AS} cells includes the sequential phosphorylation of ITAMs by active Lck (Fig. 4A of main text) and the binding of autoinhibited ZAP-70 to singly- and doubly-phosphorylated ITAMs (Fig. 4B of main text). Here, the autoinhibited ZAP-70 binds to the doubly phosphorylated ITAMs (Fig. S6) with slightly weaker affinity (K_D=96.1 nM). Next, active Lck phosphorylates tyrosines Y315 and Y319 in the ZAP-70 SH2-linker domain, leading to a ZAP-70 conformational change (to open ZAP-70), and therefore to an increase in ZAP-70 binding affinity (K_D=76.7 nM). Following this, active Lck phosphorylates the ZAP-70 catalytic domain activation loop, creating active ZAP-70. In our model for ZAP-70^{AS}+Inhibitor cells, the inhibitor keeps ZAP-70 in its open conformation, thus increasing its ITAM binding affinity (K_D=76.7 nM). It also excludes the last ZAP-70

phosphorylation step that converts ZAP-70 from the basal to the active state (since the inhibitor blocks ZAP-70 kinase activity).

Upon incorporating ZAP-70 allostery, the calculated ZAP-70 null / ZAP-70 reconstituted SILAC ratio decreases for the N- and C-terminal tyrosines within each ITAM (Fig. S6). However, the calculated ZAP-70^{AS}+Inhibitor / ZAP-70^{AS} SILAC ratio increases somewhat for both the N- and C- terminal tyrosines in ζ-chain ITAMs (Fig. S6). The calculated SILAC ratio of the ZAP-70 null / ZAP-70-reconstituted cells decreases due to ZAP-70's protective function. So, including ZAP-70 allosteric regulation can explain the experimental data on ZAP-70^{AS}+Inhibitor / ZAP-70^{AS} SILAC ratio. But, this mechanism can never allow an increase in the SILAC ratio of the ZAP-70 null / ZAP-70-reconstituted cells because this enables only the protective function of ZAP-70, which will always increase ITAM phosphorylation. Our observation that the SILAC ratio of the ZAP-70 null / ZAP-70-reconstituted cells increases for the C- terminal tyrosines led us to not explore this effect any further.

Fig. S6. (1) Description of ZAP-70 allosteric model. In the model of the ZAP-70 reconstituted and ZAP-70^{AS} cells, the autoinhibited ZAP-70 binds to the doubly phosphorylated ITAMs with weaker affinity (Kd=96.1 nM). Next, active Lck phosphorylates the tyrosine residues Y315 and Y319 in ZAP-70 SH2-linker domain, leading to ZAP-70 conformational change (to its open state), and therefore to an increase in the ZAP-70 binding affinity (Kd=76.7 nM). Later, active Lck phosphorylates the ZAP-70 catalytic domain, creating active ZAP-70. The model of ZAP-70^{AS}+Inhibitor cells keeps ZAP-70 in its autoinhibited conformation with the increased binding affinity (Kd=76.7 nM). **(2)** The results of calculations using ZAP-70 allosteric model for SILAC ratios of N- and C- terminals within each ITAM as a ratio heatmap.

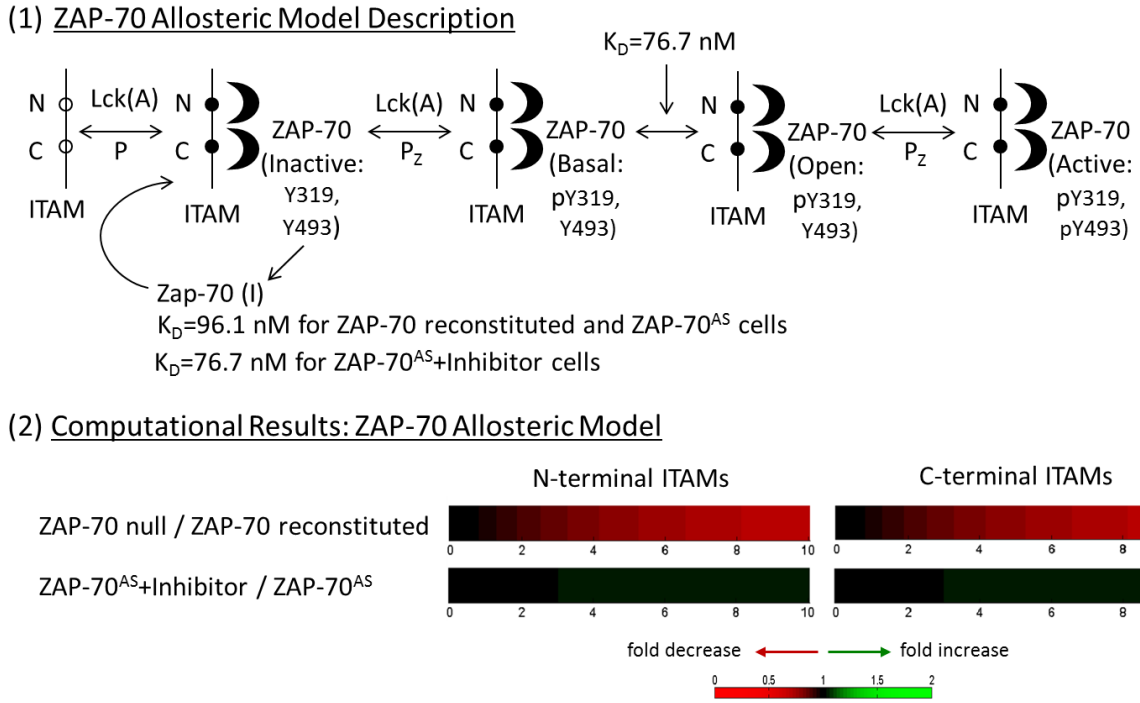

2.4 Kinetic Parameters Estimates and Sensitivity Analysis

The kinetic parameters used in our computer simulations are listed in Tables S5-S7. The rate constants for several reactions are taken from the corresponding in vitro experiments or estimated from the relevant biological experiments. However, our calculations used a few unknown kinetic parameters, for which we performed an extensive sensitivity analysis to test the robustness of our main results to a wide range of parameter variations. The results of parameter sensitivity analysis are listed in Tables S8-S12 and are illustrated in Fig. S7-S10. We varied each reaction rate and concentration parameter independently (while keeping other parameters fixed) by a large discrete change, with decreasing and increasing the parameters by several factors for concentrations and rate constants from their base value, and calculated the response from our proposed model. Many kinetic parameters variations showed no qualitative changes in our main results, revealing the robustness of our proposed model. We also identified several sensitive parameters where their variations produced some qualitative changes in our results. However, the variations of some rate constants introduced pathological biological situations, and thus were excluded.

2.4.1 Concentrations Estimates and its Sensitivity Analysis

Here we used estimates of concentrations in our calculations and subjected them to sensitivity analysis by varying each concentration by several factors from its base value. The variations of Lck, ITAM, ZAP-70 and all phosphatases concentrations in either direction had no qualitative change in our results (Tables S8 and S11).

2.4.2 Rate Constant Estimates and its Sensitivity Analysis

The rate constants for several reactions were estimated from the relevant biological experiments. The unknown rate constants were varied by several factors from their base values. The variations in many rate constants in either direction resulted in no qualitative change in our results (Tables S9, S10 and S12). The variations of several rate constants showed sensitive responses in our simulations (described in the following section). However, the variations of some rate constants introduced pathological biological situations, and were excluded from the valid parameter range. For example, ZAP-70 protects singly phosphorylated ITAMs from the phosphatases action at high k_{on} (ZAP-70 binding to the singly phosphorylated ITAMs), and competes with the Lck-SH2 binding to the singly phosphorylated ITAMs or with ZAP-70 binding to the doubly phosphorylated ITAMs (Fig. S8C and S8D, Fig. S10A and S10B, Tables S9, S10 and S12). Another pathology is observed at high k_{off} of phosphatases (all phosphatases), when the phosphatases unbind faster prior to carrying out dephosphorylation (Tables S9, S10 and S12).

2.4.3 Sensitive Kinetic Parameters

Several kinetic parameters (mainly unknown rate constants) showed sensitive responses in our simulations due to many uncertainties in the parameter values. First sensitive parameters are those for ZAP-70 negative feedback regulation (Table S9 and S10). Due to the uncertainty of these rate constants, we varied them over the several orders of magnitude to identify their valid parameter range, where they reproduce the correct biological effects. These parameters should be kept in balance with those of ZAP-70 protective function; otherwise, either biological effects can dominate and lead to the wrong conclusions. For example, if ZAP-70 protective function

dominates ZAP-70 negative feedback regulation, the SILAC ratios would decrease with time and vice versa (Fig. S7D).

The second set of sensitive parameters is for the Lck-SH2 that binds to the singly phosphorylated ITAMs and next processively phosphorylates the neighboring ITAM site. An uncertainty in these parameters is differences due to cytoplasm and membrane environments. To reproduce the experimental SILAC ratios we found that either Lck has strong kinetics in "ITAM and Lck" model, or Lck has weak kinetics in "ITAMs" model. In the "ITAM and Lck" model, Lck-SH2 strongly binds to the singly phosphorylated ITAMs (Fig. S7A and Table S9). If Lck-SH2 binds weakly, the experimental ratios are not reproduced (Fig. S7A). Furthermore, the subsequent Lck phosphorylation of neighboring site of ITAMs (while Lck-SH2 bound to ITAMs) requires increased kinetic parameters (Fig. S7B and Table S9). These high parameter values support the fact that once Lck-SH2 binds to the singly phosphorylated ITAMs, the Lck effective concentration increases, and thus promotes the phosphorylation of the neighboring site of ITAMs.

Next sensitive parameter is experimentally unknown binding affinity (K_D) of inhibited ZAP-70 to the doubly phosphorylated ITAMs in ZAP-70^{AS}+Inhibitor cells (used in the ZAP-70 allosteric model). If this binding affinity (K_D) in ZAP-70^{AS}+Inhibitor cells equals to the one in ZAP-70^{AS} cells, the ITAM phosphorylation of these two cell types would be equal (Fig. S10C and Table S12).

The last sensitive parameter is k_{cat} phosphorylating rate of the C-terminal tyrosine residues of each ITAM after phosphorylation of the singly phosphorylated N-terminal tyrosine residue of each ITAM in the "ITAMs" model. We found that this parameter should be equal or higher to the initial k_{cat} rate of the N-terminal tyrosine residue of each ITAM phosphorylation to reproduce the experimental SILAC ratios (Fig. S8B and Table S10).

2.4.4 Changes in Multiple Parameter Values

Since it is nearly impossible to explore entire parameter space, we performed sensitivity analysis by increasing or decreasing all parameters by 20% from its base values and performed the calculations for all computational models. We found that there are no qualitative changes in our results for all computational models.

2.5 Signaling Model Details

Our computational model reproduces the changes in overall ITAM phosphorylation patterns upon T cell stimulation in the absence of basal signaling. The signal strength is represented by the number of activated Lck molecules at the start of simulations. The model includes the TCR ζ-chain ITAM with two phosphorylation sites of N- and C- terminals that are sequentially phosphorylated by active Lck and sequentially dephosphorylated by phosphatases P (for example, by CD45). In our model, we represented 3 ITAM motifs of ζ-chain as a single ITAM motif since the contribution of multiple ITAMs mediated the signal amplification (as has been shown in the recent study of Dushek et al. (*21*)). Thus, an addition of two other ITAM motifs to our model would not affect our results qualitatively.

We used the following assumption in our signaling model to avoid steric hindrance between proteins, since the spacing between N- and C- terminals tyrosine residues within one ITAM is small (about 10-12 amino acids). The following molecules cannot simultaneously bind within one ITAM: two active Lck with its catalytic domains; catalytic domain of active Lck and phosphatase P; two phosphatases P; catalytic domain of active Lck and one SH2 domain of ZAP-70; catalytic domain of active Lck and SH2 domain of another active Lck. SH2 domain of active Lck and its catalytic domain can simultaneously bind to ITAM for its further processive phosphorylation. SH2 domain binding of Lck or ZAP-70 to phosphorylated ITAM occurs only at the vacant ITAM tyrosine sites. All reactions in the network use the distributive reaction mechanisms, with an exception of Lck-SH2 binding and its processive ITAM phosphorylation.

Table S5. Concentrations of species used in calculations for all models (volume = 1μm^3).

Species[*]	**No. of Molecules in V**
Lck(A)	1000
ITAM(N_0,C_0)	1000
P	2000
Z	500
P_z	500
P_{Lck}	500

[*] Lck(A) is active Lck; ITAM(N_0,C_0) is unphosphorylated ITAMs; P is phosphatases dephosphorylating singly or doubly phosphorylated ITAMs; Z is ZAP-70; P_z is phosphatases dephosphorylating basal and active ZAP-70; P_{Lck} is phosphatases dephosphorylating inactive

Lck; P_{Lck} is absent in ZAP-70 protective function ("ZAP-70 Bind" Fig. 5 of main text) and ZAP-70 allosteric models (Fig. S6).

Table S6. Reactions and kinetic parameters used in calculations for ZAP-70 negative feedback ("ZAP-70 NF" Fig. 5 of main text) model and models used to reproduce an asymmetry in ITAM phosphorylation ("ITAM & Lck" and "ITAMs" Fig. 5 of main text). Lck molecules exist in two states: active Lck(A) and inactive Lck(I). Lck(A, SH2) denotes Lck-SH2 non-catalytic domain. ITAM(N_0,C_0), ITAM(N_p,C_0), ITAM(N_0,C_p) and ITAM(N_p,C_p) molecules denote unphosphorylated ITAMs, the singly phosphorylated tyrosine residue of N-terminal or C-terminal of ITAMs, and doubly phosphorylated ITAMs, correspondingly. ZAP-70 molecules exist in three states: ZAP-70 inactive, ZAP-70 basal and ZAP-70 fully active, which are labeled by Z, Z(B) and Z(A), respectively.

Reactions	**k_{on}, molec^{-1} s^{-1}**	**k_{off}, s^{-1}**	**k_{cat}, s^{-1}**	**Reference**
Lck(A) + ITAM(N_0,C_0) ↔ [Lck(A, Nsite):ITAM(N_0,C_0)]	0.01	0.1		N/A[(1)]
[Lck(A, Nsite):ITAM(N_0,C_0)] → Lck(A) + ITAM(N_p,C_0)			0.5	k_{cat} for phosphorylation of N-terminal ITAM is 10-fold greater than k_{cat} for phosphorylation of C-terminal ITAM (*22*)
Lck(A) + ITAM(N_0,C_0) ↔ [Lck(A, Csite):ITAM(N_0,C_0)]	0.01	0.1		N/A[(1)]
[Lck(A, Csite):ITAM(N_0,C_0)] → Lck(A) + ITAM(N_0,C_p)			0.05	k_{cat} = 0.05 s^{-1} is taken from (*23*)
ITAM(N_p,C_0) + P ↔ [ITAM(N_p,C_0):P]	0.01	0.1		k_{on} = 0.01 molec^{-1}s^{-1} (0.0062 nM^{-1}s^{-1}) is taken from (*24*) k_{off} = 0.1 s^{-1} is taken from (*24*)
[ITAM(N_p,C_0):P] → ITAM(N_0,C_0) + P			0.2	k_{cat} = 0.2 s^{-1} is taken from (*23*, *24*)
ITAM(N_0,C_p) + P ↔ [ITAM(N_0,C_p):P]	0.01	0.1		k_{on} = 0.01 molec^{-1}s^{-1} (0.0062 nM^{-1}s^{-1}) is taken from (*24*) k_{off} = 0.1 s^{-1} is taken from (*24*)
[ITAM(N_0,C_p):P] → ITAM(N_0,C_0) + P			0.2	k_{cat} = 0.2 s^{-1} is taken from (*23*, *24*)
Lck(A) + ITAM(N_p,C_0) ↔ [Lck(A):ITAM(N_p,C_0)]	0.01	0.1		N/A[(1)]
[Lck(A):ITAM(N_p,C_0)] → Lck(A) + ITAM(N_p,C_p)			0.05 used in "ITAM & Lck" model;	k_{cat} = 0.05 s^{-1} is taken from (*23*)

			0.5 used in "ITAMs" model	k_{cat} = 0.5 s^{-1} is estimated from sensitivity analysis (shown in Fig. S8B)
Lck(A) + ITAM(N_0,C_p) ↔ [Lck(A):ITAM(N_0,C_p)] [Lck(A):ITAM(N_0,C_p)] → Lck(A) + ITAM(N_p,C_p)	0.01	0.1	 0.05	N/A[1] k_{cat} = 0.05 s^{-1} is taken from (*23*)
ITAM(N_p,C_p) + P ↔ [ITAM(N_p,C_p):P(Nsite)] [ITAM(N_p,C_p):P(Nsite)] → ITAM(N_0,C_p) + P	0.01	0.1	 0.2	k_{on} = 0.01 $molec^{-1}s^{-1}$ (0.0062 $nM^{-1}s^{-1}$) is taken from (*24*) k_{off} = 0.1 s^{-1} is taken from (*24*) k_{cat} = 0.2 s^{-1} is taken from (*23*, *24*)
ITAM(N_p,C_p) + P ↔ [ITAM(N_p,C_p):P(Csite)] [ITAM(N_p,C_p):P(Csite)] → ITAM(N_p,C_0) + P	0.01	0.1	 0.2	k_{on} = 0.01 $molec^{-1}s^{-1}$ (0.0062 $nM^{-1}s^{-1}$) is taken from (*24*) k_{off} = 0.1 s^{-1} is taken from (*24*) k_{cat} = 0.2 s^{-1} is taken from (*23*, *24*)
Lck(A) + ITAM(N_p,C_0)] ↔ [Lck(A, SH2):ITAM(N_p,C_0)]	0.05 used in "ITAM & Lck" model; 0.00003 used in "ITAMs" model	0.1		K_D^{exp} = 18.6 μM (*19*) We used K_D = 5 nM in "ITAM & Lck" model, which was estimated from sensitivity analysis (shown in Fig. S7A top panel). K_D^{exp} = 18.6 μM (*19*) We used K_D = 5 μM in "ITAMs" model.
[Lck(A,SH2):ITAM(N_p,C_0)]↔ [Lck(A,SH2):ITAM(N_p,C_0):Csite] [Lck(A,SH2): ITAM(N_p,C_0):Csite] → Lck(A) + ITAM(N_p,C_p)	1.0	0.1	 1.0	N/A[1] N/A[1] We have estimated these parameters from sensitivity analysis (shown in Fig. S7B top panel), based on the fact that once Lck-SH2 binds to singly phosphorylated ITAMs, Lck effective concentration increases, and thus promotes the phosphorylation of the neighboring site of ITAMs (similarly to B cells (*14*)).
Lck(A) + ITAM(N_0,C_p)] ↔ [Lck(A, SH2):ITAM(N_0,C_p)]	0.05 used in "ITAM & Lck"	0.1		K_D^{exp} = 4.7 μM (*19*) We used K_D = 5 nM in "ITAM & Lck" model, which was estimated

	model; 0.00003 used in "ITAMs" model			from sensitivity analysis (the same estimate as for N-terminal ITAMs, shown in Fig. S7A top panel). K_D^{exp} = 4.7 μM (*19*)
[Lck(A,SH2):ITAM(N_0,C_p)] ↔ [Lck(A,SH2):ITAM(N_0,C_p):Nsite] [Lck(A,SH2): ITAM(N_0,C_p):Nsite] → Lck(A) + ITAM(N_p,C_p)	1.0	0.1	 1.0	N/A[(1)] N/A[(1)] We have estimated these parameters from sensitivity analysis (the same estimate as for N-terminal ITAMs, shown in Fig. S7B top panel), based on the fact that once Lck-SH2 binds to singly phosphorylated ITAMs, Lck effective concentration increases, and thus promotes the phosphorylation of the neighboring site of ITAMs (similarly to B cells (*14*)).
ITAM(N_p,C_0) + Z ↔ [ITAM(N_p,C_0):Z]	0.00003	0.1		K_D^{exp} = 58.8 μM (*19*) We used K_D = 5 μM.
ITAM(N_0,C_p) + Z ↔ [ITAM(N_0,C_p):Z]	0.00003	0.1		K_D^{exp} = 44.5 μM (*19*) We used K_D = 5 μM.
ITAM(N_p,C_p) + Z ↔ [ITAM(N_p,C_p):Z]	0.03	0.1		K_D^{exp} = 3.5-76.6 nM (*19*, *20*) We used K_D = 5 nM.
[ITAM(N_p,C_p):Z] + Lck(A) ↔ [ITAM(N_p,C_p):Z:Lck(A)] [ITAM(N_p,C_p):Z:Lck(A)] → [ITAM(N_p,C_p):Z(B)] + Lck(A)	0.05	0.1	 0.1	N/A[(1)] The activity of ZAP-70 WT is greater than the activity of ZAP-70 Y493F mutant (*25*), thus we used k_{cat} (ZAP-70 basal) = 0.1 s^{-1} that is 4-fold lower than for active ZAP-70.
[ITAM(N_p,C_p):Z(B)] + P_z ↔ [ITAM(N_p,C_p):Z(B):P_z] [ITAM(N_p,C_p):Z(B):P_z] → [ITAM(N_p,C_p):Z] + P_z	0.01	0.1	 0.2	N/A[(1)] k_{cat}^{exp} = 0.27 s^{-1} estimated from k_{cat}^{exp}(Dephos Syk) = 0.8 s^{-1} (*26*)
[ITAM(N_p,C_p):Z(B)] + Lck(A) ↔ [ITAM(N_p,C_p):Z(B):Lck(A, SH2)]	0.05	0.1		N/A[(1)]

$[ITAM(N_p,C_p):Z(B):Lck(A, SH2)] \rightarrow [ITAM(N_p,C_p):Z(A)] + Lck(A)$			0.4	k_{cat}^{exp}(Syk) = 0.5-0.9 s^{-1} (*24*, *26*); k_{cat}^{exp}(ZAP-70) is 3-fold lower than k_{cat}^{exp}(Syk) (*26*), resulting in k_{cat}(ZAP-70) = 0.3 s^{-1}
$[ITAM(N_p,C_p):Z(A)] + P_z \leftrightarrow [ITAM(N_p,C_p):Z(A):P_z]$ $[ITAM(N_p,C_p):Z(A):P_z] \rightarrow [ITAM(N_p,C_p):Z(B)] + P_z$	0.01	0.1	 0.2	N/A[(1)] k_{cat}^{exp} = 0.27 s^{-1} estimated from k_{cat}^{exp}(Dephos Syk) = 0.8 s^{-1} (*26*)
$Lck(A) + [ITAM(N_p,C_p):Z(A)] \leftrightarrow [Lck(A):ITAM(N_p,C_p):Z(A)]$ $[Lck(A):ITAM(N_p,C_p):Z(A)] \rightarrow Lck(I) + [ITAM(N_p,C_p):Z(A)]$	0.0025	0.1	 0.02 used in "ITAM & Lck" model; 0.05 used in "ITAMs" model	N/A[(1)] N/A[(1)] We have estimated these parameters from sensitivity analysis (shown in Fig. S7C and Fig. S7D top panels), based on the fact that tyrosine Y192 site of Lck is a negative regulatory site observed in the current ZAP-70^{AS}+Inhibitor / ZAP-70^{AS} SILAC experiments (shown in Table 1 of main text).
$Lck(A) + [ITAM(N_p,C_p):Z(B) \leftrightarrow [Lck(A):ITAM(N_p,C_p):Z(B)]$ $[Lck(A):ITAM(N_p,C_p):Z(B)] \rightarrow Lck(I) + [ITAM(N_p,C_p):Z(B)]$	0.0025	0.1	 0.02 used in "ITAM & Lck" model; 0.05 used in "ITAMs" model	N/A[(1)] N/A[(1)] We have estimated these parameters from sensitivity analysis (the same estimates as for ZAP-70(A), shown in Fig. S7C and Fig. S7D top panels), based on the fact that tyrosine Y192 site of Lck is a negative regulatory site observed in the current ZAP-70^{AS}+Inhibitor / ZAP-70^{AS} SILAC experiments (shown in Table 1 of main text).
$Lck(I) + P_{Lck} \leftrightarrow [Lck(I):P_{Lck}]$	0.015 used in "ITAM & Lck" model; 0.0015 used in	0.1		N/A[(1)] N/A[(1)]

$[Lck(I):P_{Lck}] \rightarrow Lck(A) + P_{Lck}$	"ITAMs" model		0.001 used in "ITAM & Lck" model; 0.0001 used in "ITAMs" model;	N/A[(1)]

[(1)] Not available. We have estimated these numbers by performing sensitivity analysis of initially guessed kinetic parameters used in calculations.

Table S7. Reactions and kinetic parameters used in calculations for ZAP-70 allosteric model. Active Lck is denoted by Lck(A). ITAM(N_0,C_0), ITAM(N_p,C_0), ITAM(N_0,C_p) and ITAM(N_p,C_p) molecules denote unphosphorylated ITAMs, the singly phosphorylated tyrosine residue of N-terminal or C-terminal of ITAMs, and doubly phosphorylated ITAMs, correspondingly. ZAP-70 molecules exist in three states: ZAP-70 inactive, ZAP-70 basal and ZAP-70 fully active, which are labeled by Z, Z(B) and Z(A), respectively.

Reactions	**k_{on}, molec^{-1} s^{-1}**	**k_{off}, s^{-1}**	**k_{cat}, s^{-1}**	**Reference**
$Lck(A) + ITAM(N_0,C_0) \leftrightarrow [Lck(A, Nsite):ITAM(N_0,C_0)]$	0.01	0.1		N/A[(1)]
$[Lck(A, Nsite):ITAM(N_0,C_0)] \rightarrow Lck(A) + ITAM(N_p,C_0)$			0.05	k_{cat} = 0.05 s^{-1} is taken from (*23*)
$Lck(A) + ITAM(N_0,C_0) \leftrightarrow [Lck(A, Csite):ITAM(N_0,C_0)]$	0.01	0.1		N/A[(1)]
$[Lck(A, Csite):ITAM(N_0,C_0)] \rightarrow Lck(A) + ITAM(N_0,C_p)$			0.05	k_{cat} = 0.05 s^{-1} is taken from (*23*)
$ITAM(N_p,C_0) + P \leftrightarrow [ITAM(N_p,C_0):P]$	0.01	0.1		k_{on} = 0.01 molec^{-1}s^{-1} (0.0062 nM^{-1}s^{-1}) is taken from (*24*)
				k_{off} = 0.1 s^{-1} is taken from (*24*)
$[ITAM(N_p,C_0):P] \rightarrow ITAM(N_0,C_0) + P$			0.2	k_{cat} = 0.2 s^{-1} is taken from (*23*, *24*)
$ITAM(N_0,C_p) + P \leftrightarrow [ITAM(N_0,C_p):P]$	0.01	0.1		k_{on} = 0.01 molec^{-1}s^{-1} (0.0062 nM^{-1}s^{-1}) is taken from (*24*)
				k_{off} = 0.1 s^{-1} is taken from (*24*)
$[ITAM(N_0,C_p):P] \rightarrow ITAM(N_0,C_0) + P$			0.2	k_{cat} = 0.2 s^{-1} is taken from (*23*, *24*)
$Lck(A) + ITAM(N_p,C_0) \leftrightarrow [Lck(A):ITAM(N_p,C_0)]$	0.01	0.1		N/A[(1)]

$[Lck(A):ITAM(N_p,C_0)] \rightarrow Lck(A) + ITAM(N_p,C_p)$			0.05	k_{cat} = 0.05 s^{-1} is taken from (*23*)
$Lck(A) + ITAM(N_0,C_p) \leftrightarrow [Lck(A):ITAM(N_0,C_p)]$ $[Lck(A):ITAM(N_0,C_p)] \rightarrow Lck(A) + ITAM(N_p,C_p)$	0.01	0.1	 0.05	N/A[(1)] k_{cat} = 0.05 s^{-1} is taken from (*23*)
$ITAM(N_p,C_p) + P \leftrightarrow [ITAM(N_p,C_p):P(Nsite)]$ $[ITAM(N_p,C_p):P(Nsite)] \rightarrow ITAM(N_0,C_p) + P$	0.01	0.1	 0.2	k_{on} = 0.01 $molec^{-1}s^{-1}$ (0.0062 $nM^{-1}s^{-1}$) is taken from (*24*) k_{off} = 0.1 s^{-1} is taken from (*24*) k_{cat} = 0.2 s^{-1} is taken from (*23*, *24*)
$ITAM(N_p,C_p) + P \leftrightarrow [ITAM(N_p,C_p):P(Csite)]$ $[ITAM(N_p,C_p):P(Csite)] \rightarrow ITAM(N_p,C_0) + P$	0.01	0.1	 0.2	k_{on} = 0.01 $molec^{-1}s^{-1}$ (0.0062 $nM^{-1}s^{-1}$) is taken from (*24*) k_{off} = 0.1 s^{-1} is taken from (*24*) k_{cat} = 0.2 s^{-1} is taken from (*23*, *24*)
$ITAM(N_p,C_0) + Z \leftrightarrow [ITAM(N_p,C_0):Z]$ $ITAM(N_0,C_p) + Z \leftrightarrow [ITAM(N_0,C_p):Z]$ $ITAM(N_p,C_p) + Z \leftrightarrow [ITAM(N_p,C_p):Z]$	0.00003 0.00003 0.00173 used for ZAP-70 reconstituted and ZAP-70^{AS} cells; 0.00217 used for ZAP-70^{AS}+Inhibitor cells	0.1 0.1 0.1		K_D^{exp} = 58.8 µM (*19*) We used K_D = 5 µM. K_D^{exp} = 44.5 µM (*19*) We used K_D = 5 µM. K_D^{exp} (ZAP-70 Y315F Y319F) = 96.1 nM (*20*) K_D^{exp} (ZAP-70 WT) = 76.6 nM (*20*)
$[ITAM(N_p,C_p):Z] + Lck(A) \leftrightarrow [ITAM(N_p,C_p):Z:Lck(A)]$ $[ITAM(N_p,C_p):Z:Lck(A)] \rightarrow [ITAM(N_p,C_p):Z(B)] + Lck(A)$	0.05	0.1	 0.1	N/A[(1)] The activity of ZAP-70 WT is greater than the activity of ZAP-70 Y493F mutant (*25*), thus we used k_{cat} (ZAP-70 basal) = 0.1 s^{-1} that is 4-fold lower than for active ZAP-70.
$[ITAM(N_p,C_p):Z(B)] + P_z \leftrightarrow [ITAM(N_p,C_p):Z(B):P_z]$ $[ITAM(N_p,C_p):Z(B):P_z] \rightarrow [ITAM(N_p,C_p):Z] + P_z$	0.01	0.1	 0.2	N/A[(1)] k_{cat}^{exp} = 0.27 s^{-1} estimated from k_{cat}^{exp}(Dephos Syk) = 0.8 s^{-1} (*26*)
$[ITAM(N_p,C_p):Z(B)] \leftrightarrow [ITAM(N_p,C_p):Z(B, open)]$	0.00217	0.1		K_D^{exp} (ZAP-70 WT) =

				76.6 nM (*20*)
$[ITAM(N_p,C_p):Z(B, open)] + Lck(A) \leftrightarrow [ITAM(N_p,C_p):Z(B, open):Lck(A, SH2)]$ $[ITAM(N_p,C_p):Z(B, open):Lck(A, SH2)] \rightarrow [ITAM(N_p,C_p):Z(A)] + Lck(A)$	0.05	0.1	0.4	N/A[(1)] k_{cat}^{exp}(Syk) = 0.5-0.9 s^{-1} (*24*, *26*); k_{cat}^{exp}(ZAP-70) is 3-fold lower than k_{cat}^{exp}(Syk) (*26*), resulting in k_{cat}(ZAP-70) = 0.3 s^{-1}
$[ITAM(N_p,C_p):Z(A)] + P_z \leftrightarrow [ITAM(N_p,C_p):Z(A):P_z]$ $[ITAM(N_p,C_p):Z(A):P_z] \rightarrow [ITAM(N_p,C_p):Z(B, open)] + P_z$	0.01	0.1	0.2	N/A[(1)] k_{cat}^{exp} = 0.27 s^{-1} estimated from k_{cat}^{exp}(Dephos Syk) = 0.8 s^{-1} (*26*)
$[ITAM(N_p,C_p):Z(B, open)] + P_z \leftrightarrow [ITAM(N_p,C_p):Z(B, open):P_z]$ $[ITAM(N_p,C_p):Z(B, open):P_z] \rightarrow [ITAM(N_p,C_p):Z] + P_z$	0.01	0.1	0.2	N/A[(1)] k_{cat}^{exp} = 0.27 s^{-1} estimated from k_{cat}^{exp}(Dephos Syk) = 0.8 s^{-1} (*26*)

[(1)] Not available. We have estimated these numbers by performing sensitivity analysis of initially guessed kinetic parameters used in calculations.

Table S8. Sensitivity analysis of concentrations of signaling molecules used in calculations for "ITAM & Lck" and "ITAMs" models. The variation of number of molecules for every species was in the following parameter range: 100, 500, 1000, 1500, 2000 molecules.

Species*	**Valid Parameter Range (no. of molecules)**	**Result**
Lck(A)	greater than 500	no qualitative change
$ITAM(N_0,C_0)$	greater than 500	no qualitative change
P	greater than 100	no qualitative change
Z	greater than 100 and less than 1000 in "ITAM & Lck" model; all range in "ITAMs" model	no qualitative change
P_z	greater than 100 and less than 1000	no qualitative change at high concentration: all ZAP-70 is dephosphorylated and ZAP-70 protective function dominates
P_{Lck}	greater than 100 in "ITAM & Lck" model; all range in "ITAMs" model	no qualitative change

* Lck(A) is active Lck; $ITAM(N_0,C_0)$ is unphosphorylated ITAMs; P is phosphatases dephosphorylating singly and doubly phosphorylated ITAMs; Z is ZAP-70; P_z is phosphatases dephosphorylating basal and active ZAP-70; P_{Lck} is phosphatases dephosphorylating inactive

Lck.

Table S9. Sensitivity analysis of kinetic parameters used in calculations for "ITAM & Lck" model. The variation of kinetic parameters for every chemical reaction was in the following parameter range: 0.001, 0.01, 0.1, 0.5, 1.0, 3.0, 5.0 s^{-1}. Lck molecules exist in two states: active Lck(A) and inactive Lck(I). Lck(A, SH2) denotes Lck-SH2 non-catalytic domain. ITAM(N_0,C_0), ITAM(N_p,C_0), ITAM(N_0,C_p) and ITAM(N_p,C_p) molecules denote unphosphorylated ITAMs, the singly phosphorylated tyrosine residue of N-terminal or C-terminal of ITAMs, and doubly phosphorylated ITAMs, correspondingly. ZAP-70 molecules exist in three states: ZAP-70 inactive, ZAP-70 basal and ZAP-70 fully active, which are labeled by Z, Z(B) and Z(A), respectively.

Reactions	**Valid Parameter Range** (k_{on} $molec^{-1}s^{-1}$; k_{off}, k_{cat} s^{-1})	**Result**
Lck(A) + ITAM(N_0,C_0) ↔ [Lck(A, Nsite):ITAM(N_0,C_0)]	k_{on}: greater than 0.001 k_{off}: less than 1.0	k_{on}: no qualitative change k_{off}: no qualitative change
[Lck(A, Nsite):ITAM(N_0,C_0)] → Lck(A) + ITAM(N_p,C_0)	greater than 0.1	no qualitative change
Lck(A) + ITAM(N_0,C_0) ↔ [Lck(A, Csite):ITAM(N_0,C_0)]	k_{on}: less than 0.1 k_{off}: greater than 0.01	k_{on}: no qualitative change k_{off}: no qualitative change
[Lck(A, Csite):ITAM(N_0,C_0)] → Lck(A) + ITAM(N_0,C_p)	greater than 0.01	no qualitative change
ITAM(N_p,C_0) + P ↔ [ITAM(N_p,C_0):P]	k_{on}: less than 0.1 k_{off}: all range	k_{on}: no qualitative change k_{off}: no qualitative change
[ITAM(N_p,C_0):P] → ITAM(N_0,C_0) + P	less than 0.5	no qualitative change
ITAM(N_0,C_p) + P ↔ [ITAM(N_0,C_p):P]	k_{on}: less than 0.1 k_{off}: all range	k_{on}: no qualitative change k_{off}: no qualitative change
[ITAM(N_0,C_p):P] → ITAM(N_0,C_0) + P	greater than 0.01	no qualitative change
Lck(A) + ITAM(N_p,C_0) ↔ [Lck(A):ITAM(N_p,C_0)]	k_{on}: less than 0.1 k_{off}: greater than 0.01	k_{on}: no qualitative change k_{off}: no qualitative change
[Lck(A):ITAM(N_p,C_0)] → Lck(A) + ITAM(N_p,C_p)	all range	no qualitative change
Lck(A) + ITAM(N_0,C_p) ↔ [Lck(A):ITAM(N_0,C_p)]	k_{on}: all range k_{off}: less than 0.1	k_{on}: no qualitative change k_{off}: no qualitative change
[Lck(A):ITAM(N_0,C_p)] → Lck(A) + ITAM(N_p,C_p)	less than 0.1	no qualitative change
ITAM(N_p,C_p) + P ↔ [ITAM(N_p,C_p):P(Nsite)]	k_{on}: greater than 0.01 k_{off}: less than 0.5	k_{on}: no qualitative change k_{off}: no qualitative change
[ITAM(N_p,C_p):P(Nsite)] → ITAM(N_0,C_p) + P	greater than 0.1 and less than 0.5	no qualitative change
ITAM(N_p,C_p) + P ↔ [ITAM(N_p,C_p):P(Csite)]	k_{on}: less than 0.1 k_{off}: greater than 0.01	k_{on}: no qualitative change k_{off}: no qualitative change
[ITAM(N_p,C_p):P(Csite)] → ITAM(N_p,C_0) + P	greater than 0.1 and less than 0.5	no qualitative change
Lck(A) + ITAM(N_p,C_0)] ↔ [Lck(A, SH2):ITAM(N_p,C_0)]	k_{on}: greater than 0.01 and less than 0.1 k_{off}: less than 1.0	k_{on}: no qualitative change (shown in Fig. S7A top panel) k_{off}: no qualitative change;

		at high rates the N-terminal ZAP-70 null / ZAP-70 reconstituted SILAC ratio is greater than C-terminal one
[Lck(A,SH2):ITAM(N_p,C_0)] ↔ [Lck(A,SH2):ITAM(N_p,C_0):Csite]	k_{on}: greater than or equals to 0.5 k_{off}: less than 1.0	k_{on}: no qualitative change (shown in Fig. S7B top panel) k_{off}: no qualitative change; at high rates the N-terminal ZAP-70 null / ZAP-70 reconstituted SILAC ratio is greater than C-terminal one
[Lck(A,SH2):ITAM(N_p,C_0):Csite] → Lck(A) + ITAM(N_p,C_p)	greater than or equals to 0.5	no qualitative change
Lck(A) + ITAM(N_0,C_p)] ↔ [Lck(A, SH2):ITAM(N_0,C_p)]	k_{on}: less than 0.1 k_{off}: all range	k_{on}: no qualitative change k_{off}: no qualitative change
[Lck(A,SH2):ITAM(N_0,C_p)] ↔ [Lck(A,SH2):ITAM(N_0,C_p):Nsite]	k_{on}: all range k_{off}: all range	k_{on}: no qualitative change k_{off}: no qualitative change
[Lck(A,SH2):ITAM(N_0,C_p):Nsite] → Lck(A) + ITAM(N_p,C_p)	all range	no qualitative change
ITAM(N_p,C_0) + Z ↔ [ITAM(N_p,C_0):Z]	k_{on}: less than 0.01 k_{off}: all range	k_{on}: at high rates - observed artifact: N-terminal ITAMs protected by ZAP-70 from dephosphorylation by phosphatases, causing decreased phosphorylation of C-terminal ITAMs in ZAP-70 reconstituted cells (shown in Fig. S8C) k_{off}: no qualitative change
ITAM(N_0,C_p) + Z ↔ [ITAM(N_0,C_p):Z]	k_{on}: less than 0.01 k_{off}: all range	k_{on}: at high rates - observed artifact: C-terminal ITAMs protected by ZAP-70 from dephosphorylation by phosphatases, causing decreased phosphorylation of N-terminal ITAMs in ZAP-70 reconstituted cells (shown in Fig. S8D) k_{off}: no qualitative change
ITAM(N_p,C_p) + Z ↔ [ITAM(N_p,C_p):Z]	k_{on}: less than 0.1 k_{off}: all range	k_{on}: at high rates ZAP-70 protective function dominates over ZAP-70 negative feedback k_{off}: no qualitative change
[ITAM(N_p,C_p):Z] + Lck(A) ↔ [ITAM(N_p,C_p):Z:Lck(A)]	k_{on}: all range k_{off}: all range	k_{on}: no qualitative change k_{off}: no qualitative change
[ITAM(N_p,C_p):Z:Lck(A)] → [ITAM(N_p,C_p):Z(B)] + Lck(A)	greater than 0.01 and less than 0.1	no qualitative change
[ITAM(N_p,C_p):Z(B)] + P_z ↔ [ITAM(N_p,C_p):Z(B):P_z]	k_{on}: greater than 0.001 and less than 0.1 k_{off}: less than 0.5	k_{on}: no qualitative change k_{off}: no qualitative change;

		at high rates – opposite trend: N- and C- terminal ITAM phosphorylation of ZAP-70AS cells is greater than in ZAP-70AS+Inhibitor cells, since phosphatases unbind before its subsequent dephosphorylation, causing an increased contribution from ZAP-70 basal state in both cell types
$[ITAM(N_p,C_p):Z(B):P_z] \rightarrow [ITAM(N_p,C_p):Z] + P_z$	greater than 0.01	no qualitative change
$[ITAM(N_p,C_p):Z(B)] + Lck(A) \leftrightarrow [ITAM(N_p,C_p):Z(B):Lck(A, SH2)]$	k_{on}: all range k_{off}: all range	k_{on}: no qualitative change k_{off}: no qualitative change
$[ITAM(N_p,C_p):Z(B):Lck(A, SH2)] \rightarrow [ITAM(N_p,C_p):Z(A)] + Lck(A)$	greater than 0.1	no qualitative change
$[ITAM(N_p,C_p):Z(A)] + P_z \leftrightarrow [ITAM(N_p,C_p):Z(A):P_z]$	k_{on}: greater than 0.001 and less than or equals to 0.01 k_{off}: less than 0.5	k_{on}: no qualitative change k_{off}: no qualitative change
$[ITAM(N_p,C_p):Z(A):P_z] \rightarrow [ITAM(N_p,C_p):Z(B)] + P_z$	greater than 0.1	no qualitative change
$Lck(A) + [ITAM(N_p,C_p):Z(A)] \leftrightarrow [Lck(A):ITAM(N_p,C_p):Z(A)]$	k_{on}: greater than or equals to 0.001 and less than 0.01 k_{off}: less than 0.5	k_{on}: there is no qualitative change within this valid parameter range (shown in Fig. S7C top panel) k_{off}: no qualitative change; at high rates ZAP-70 unbinds faster before its subsequent catalysis, making ZAP-70 protective function stronger than ZAP-70 negative feedback regulation
$[Lck(A):ITAM(N_p,C_p):Z(A)] \rightarrow Lck(I) + [ITAM(N_p,C_p):Z(A)]$	greater than 0.01 and less than 0.1	no qualitative change; at high rates ZAP-70 negative feedback dominates (shown in Fig. S7D top panel)
$Lck(A) + [ITAM(N_p,C_p):Z(B) \leftrightarrow [Lck(A):ITAM(N_p,C_p):Z(B)]$	k_{on}: greater than 0.001 and less than 0.1 k_{off}: greater than 0.01	k_{on}: no qualitative change k_{off}: no qualitative change
$[Lck(A):ITAM(N_p,C_p):Z(B)] \rightarrow Lck(I) + [ITAM(N_p,C_p):Z(B)]$	less than 0.1	no qualitative change
$Lck(I) + P_{Lck} \leftrightarrow [Lck(I):P_{Lck}]$	k_{on}: all range k_{off}: all range	k_{on}: no qualitative change k_{off}: no qualitative change
$[Lck(I):P_{Lck}] \rightarrow Lck(A) + P_{Lck}$	less than or equals to 0.001	at high rates the negative feedback is weak and the ZAP-70 protective function dominates

Fig. S7. Sensitivity analysis of kinetic parameters used in calculations for "ITAM & Lck" model. The variation of kinetic parameters for every chemical reaction was in the following parameter range: 0.001, 0.01, 0.1, 0.5, 1.0, 3.0, 5.0 s^{-1}.

(A) Sensitivity analysis for varying k_{on} rate of binding Lck-SH2 to the singly phosphorylated tyrosine residue of N-terminal ITAMs (Lck(A) + ITAM(N_p,C_0) ↔ [Lck(A, SH2):ITAM(N_p,C_0)] reaction). For ZAP-70 null / ZAP-70 reconstituted SILAC ratio (top panel figures): at low rates ZAP-70 null / ZAP-70 reconstituted ratio for C-terminal ITAMs is lower than ratio for N-terminal ITAMs; at high rates an asymmetry of ITAM phosphorylation is reproduced. For ZAP-70^{AS}+Inhibitor / ZAP-70^{AS} SILAC ratio (bottom panel figures): there is no qualitative change.

(B) Sensitivity analysis for varying k_{on} rate of binding Lck to the C-terminal ITAMs while bound with its SH2 domain to singly phosphorylated N-terminal ITAMs ([Lck(A,SH2):ITAM(N_p,C_0)] ↔ [Lck(A,SH2):ITAM(N_p,C_0):Csite] reaction). For ZAP-70 null / ZAP-70 reconstituted SILAC ratio (top panel figures): at low rates ZAP-70 null / ZAP-70 reconstituted ratio for C-terminal ITAMs is lower than ratio for N-terminal ITAMs; at high rates an asymmetry of ITAM phosphorylation is reproduced. For ZAP-70^{AS}+Inhibitor / ZAP-70^{AS} SILAC ratio (bottom panel figures): there is no qualitative change. These parameters support the observation that, once Lck-SH2 binds to the singly phosphorylated ITAMs, the Lck effective concentration increases, and thus promotes the phosphorylation of the neighboring site of ITAMs.

(C) Sensitivity analysis for varying k_{on} rate of binding of ZAP-70 bound ITAM complex to active Lck (Lck(A) + [ITAM(N_p,C_p):Z(A)] ↔ [Lck(A):ITAM(N_p,C_p):Z(A)] reaction). For both SILAC ratios: at high rates negative feedback dominates; at low rates the experimental trends are reproduced.

(D) Sensitivity analysis for varying k_{cat} rate for ZAP-70 negative feedback regulation of Lck at Y192 site ([Lck(A):ITAM(N_p,C_p):Z(A)] → Lck(I) + [ITAM(N_p,C_p):Z(A)] reaction). For both SILAC ratios: at low rates ZAP-70 protective function dominates; at high rates the negative feedback dominates and the experimental trends are reproduced.

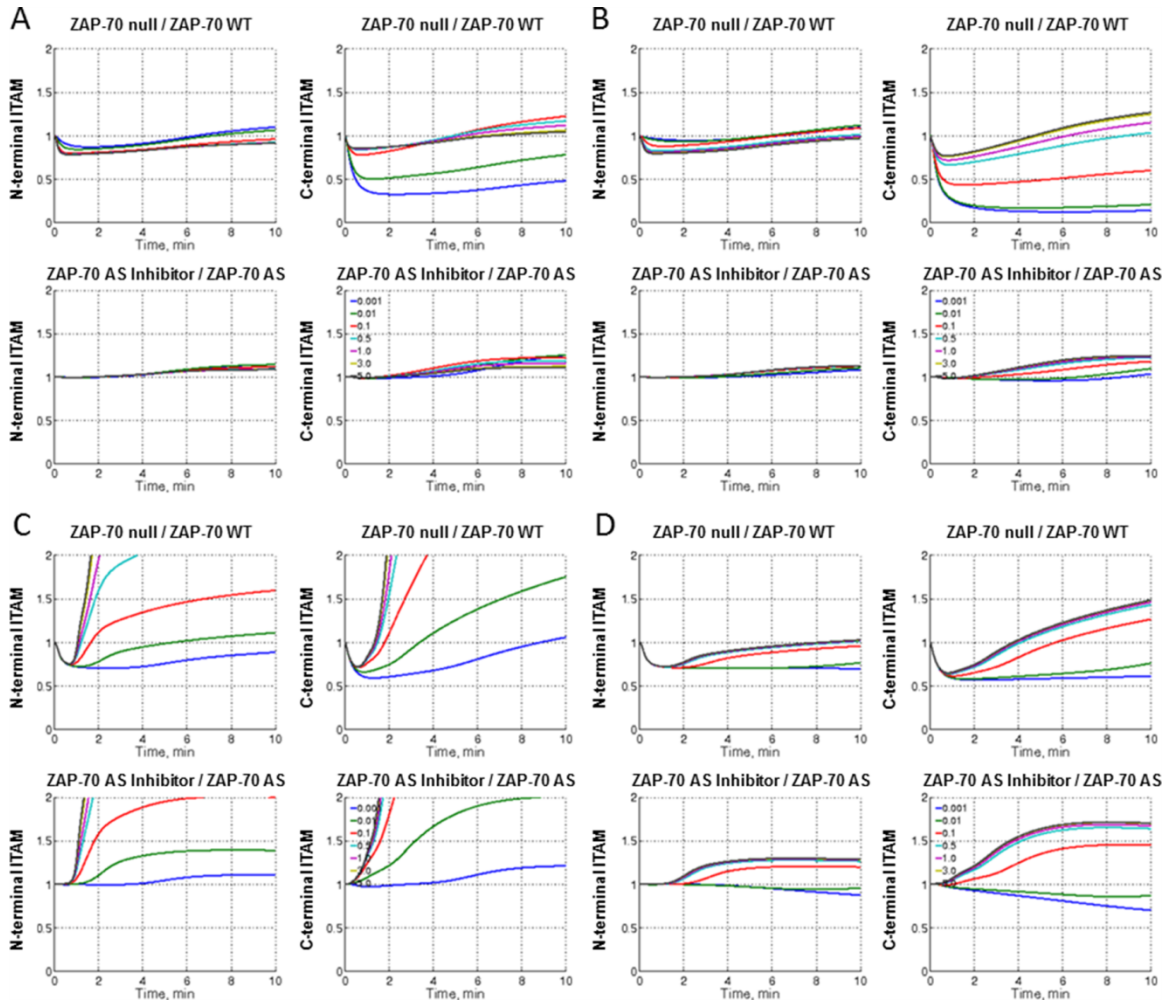

Table S10. Sensitivity analysis of kinetic parameters used in calculations for "ITAMs" model. The variation of kinetic parameters for every chemical reaction was in the following parameter range: 0.001, 0.01, 0.1, 0.5, 1.0, 3.0, 5.0 s^{-1}. Lck molecules exist in two states: active Lck(A) and inactive Lck(I). ITAM(N_0,C_0), ITAM(N_p,C_0), ITAM(N_0,C_p) and ITAM(N_p,C_p) molecules denote unphosphorylated ITAMs, the singly phosphorylated tyrosine residue of N-terminal or C-terminal of ITAMs, and doubly phosphorylated ITAMs, correspondingly. ZAP-70 molecules exist in three states: ZAP-70 inactive, ZAP-70 basal and ZAP-70 fully active, which are labeled by Z, Z(B) and Z(A), respectively.

Reactions	**Valid Parameter Range (k_{on} $molec^{-1}s^{-1}$; k_{off}, k_{cat} s^{-1})**	**Result**

$Lck(A) + ITAM(N_0,C_0) \leftrightarrow [Lck(A, Nsite):ITAM(N_0,C_0)]$	k_{on}: greater than or equals to 0.01 k_{off}: less than 0.5	k_{on}: no qualitative change k_{off}: no qualitative change
$[Lck(A, Nsite):ITAM(N_0,C_0)] \rightarrow Lck(A) + ITAM(N_p,C_0)$	greater than 0.1	at low rates ZAP-70 null / ZAP-70 reconstituted ratio for N-terminal ITAM is lower than ratio for C-terminal ITAM, since k_{cat} for phosphorylation of C-terminal ITAM is higher (shown in Fig. S8A)
$Lck(A) + ITAM(N_0,C_0) \leftrightarrow [Lck(A, Csite):ITAM(N_0,C_0)]$	k_{on}: greater than or equals to 0.01 k_{off}: less than 0.5	k_{on}: no qualitative change k_{off}: no qualitative change
$[Lck(A, Csite):ITAM(N_0,C_0)] \rightarrow Lck(A) + ITAM(N_0,C_p)$	greater than 0.01	no qualitative change; at high rates ZAP-70 null / ZAP-70 reconstituted ratio for C-terminal ITAM is greater than ratio for N-terminal ITAM, since k_{cat} for phosphorylation of C-terminal ITAM is higher
$ITAM(N_p,C_0) + P \leftrightarrow [ITAM(N_p,C_0):P]$	k_{on}: less than 0.1 k_{off}: all range	k_{on}: no qualitative change k_{off}: no qualitative change
$[ITAM(N_p,C_0):P] \rightarrow ITAM(N_0,C_0) + P$	greater than 0.01	no qualitative change
$ITAM(N_0,C_p) + P \leftrightarrow [ITAM(N_0,C_p):P]$	k_{on}: less than 0.1 k_{off}: all range	k_{on}: no qualitative change k_{off}: no qualitative change
$[ITAM(N_0,C_p):P] \rightarrow ITAM(N_0,C_0) + P$	less than 0.5	no qualitative change
$Lck(A) + ITAM(N_p,C_0) \leftrightarrow [Lck(A):ITAM(N_p,C_0)]$	k_{on}: greater than 0.001 k_{off}: less than or equals to 0.5	k_{on}: no qualitative change k_{off}: no qualitative change
$[Lck(A):ITAM(N_p,C_0)] \rightarrow Lck(A) + ITAM(N_p,C_p)$	greater than 0.1	at low rates ZAP-70 null / ZAP-70 reconstituted ratio for N-terminal ITAM is greater than ratio for C-terminal ITAM (shown in Fig. S8B)
$Lck(A) + ITAM(N_0,C_p) \leftrightarrow [Lck(A):ITAM(N_0,C_p)]$	k_{on}: greater than 0.001 k_{off}: less than 1.0	k_{on}: no qualitative change k_{off}: no qualitative change
$[Lck(A):ITAM(N_0,C_p)] \rightarrow Lck(A) + ITAM(N_p,C_p)$	less than 0.5	no qualitative change
$ITAM(N_p,C_p) + P \leftrightarrow [ITAM(N_p,C_p):P(Nsite)]$	k_{on}: less than 0.5 k_{off}: all range	k_{on}: no qualitative change k_{off}: no qualitative change
$[ITAM(N_p,C_p):P(Nsite)] \rightarrow ITAM(N_0,C_p) + P$	greater than to 0.1	no qualitative change
$ITAM(N_p,C_p) + P \leftrightarrow [ITAM(N_p,C_p):P(Csite)]$	k_{on}: less than 0.5 k_{off}: all range	k_{on}: no qualitative change k_{off}: no qualitative change
$[ITAM(N_p,C_p):P(Csite)] \rightarrow ITAM(N_p,C_0) + P$	less than 0.5	no qualitative change
$ITAM(N_p,C_0) + Z \leftrightarrow [ITAM(N_p,C_0):Z]$	k_{on}: less than 0.01	k_{on}: at high rates - observed artifact: N-terminal ITAMs protected by ZAP-70 from dephosphorylation by phosphatases, causing decreased phosphorylation of C-terminal ITAMs in

		ZAP-70 reconstituted cells (shown in Fig. S8C)
	k_{off}: all range	k_{off}: no qualitative change
$ITAM(N_0,C_p) + Z \leftrightarrow [ITAM(N_0,C_p):Z]$	k_{on}: less than 0.01	k_{on}: at high rates - observed artifact: C-terminal ITAMs protected by ZAP-70 from dephosphorylation by phosphatases, causing decreased phosphorylation of N-terminal ITAMs in ZAP-70 reconstituted cells (shown in Fig. S8D)
	k_{off}: all range	k_{off}: no qualitative change
$ITAM(N_p,C_p) + Z \leftrightarrow [ITAM(N_p,C_p):Z]$	k_{on}: less than 0.5	k_{on}: at high rates ZAP-70 protective function dominates over ZAP-70 negative feedback
	k_{off}: greater than 0.01	k_{off}: no qualitative change
$[ITAM(N_p,C_p):Z] + Lck(A) \leftrightarrow [ITAM(N_p,C_p):Z:Lck(A)]$	k_{on}: less than 0.1	k_{on}: no qualitative change; at high rates – ZAP-70 protective function dominates
	k_{off}: all range	k_{off}: no qualitative change
$[ITAM(N_p,C_p):Z:Lck(A)] \rightarrow [ITAM(N_p,C_p):Z(B)] + Lck(A)$	greater than 0.01 and less than 0.1	no qualitative change
$[ITAM(N_p,C_p):Z(B)] + P_z \leftrightarrow [ITAM(N_p,C_p):Z(B):P_z]$	k_{on}: greater than or equals to 0.01 and less than 0.1	k_{on}: no qualitative change
	k_{off}: less than 0.5	k_{off}: no qualitative change
$[ITAM(N_p,C_p):Z(B):P_z] \rightarrow [ITAM(N_p,C_p):Z] + P_z$	greater than 0.01	no qualitative change
$[ITAM(N_p,C_p):Z(B)] + Lck(A) \leftrightarrow$ $[ITAM(N_p,C_p):Z(B):Lck(A, SH2)]$	k_{on}: greater than 0.001 and less than 1.0	k_{on}: no qualitative change
	k_{off}: less than 3.0	k_{off}: no qualitative change
$[ITAM(N_p,C_p):Z(B):Lck(A, SH2)] \rightarrow$ $[ITAM(N_p,C_p):Z(A)] + Lck(A)$	greater than 0.1	no qualitative change
$[ITAM(N_p,C_p):Z(A)] + P_z \leftrightarrow [ITAM(N_p,C_p):Z(A):P_z]$	k_{on}: greater than 0.001 and less than or equals to 0.01	k_{on}: no qualitative change
	k_{off}: less than or equals to 0.5	k_{off}: no qualitative change
$[ITAM(N_p,C_p):Z(A):P_z] \rightarrow [ITAM(N_p,C_p):Z(B)] + P_z$	greater than or equals to 0.1	no qualitative change
$Lck(A) + [ITAM(N_p,C_p):Z(A)] \leftrightarrow$ $[Lck(A):ITAM(N_p,C_p):Z(A)]$	k_{on}: greater than or equals to 0.001 and less than 0.01	k_{on}: no qualitative change
	k_{off}: less than 0.5	k_{off}: no qualitative change
$[Lck(A):ITAM(N_p,C_p):Z(A)] \rightarrow$ $Lck(I) + [ITAM(N_p,C_p):Z(A)]$	greater than 0.01	no qualitative change
$Lck(A) + [ITAM(N_p,C_p):Z(B) \leftrightarrow$ $[Lck(A):ITAM(N_p,C_p):Z(B)]$	k_{on}: greater than 0.001 and less than 0.1	k_{on}: no qualitative change
	k_{off}: greater than 0.01	k_{off}: no qualitative change

[Lck(A):ITAM(N_p,C_p):Z(B)] → Lck(I) + [ITAM(N_p,C_p):Z(B)]	greater than 0.01 and less than 0.5	no qualitative change
Lck(I) + P_{Lck} ↔ [Lck(I):P_{Lck}]	k_{on}: all range k_{off}: all range	k_{on}: no qualitative change k_{off}: no qualitative change
[Lck(I):P_{Lck}] → Lck(A) + P_{Lck}	less than 0.001	at high rates the negative feedback is weak and the ZAP-70 protective function dominates

Fig. S8. Sensitivity analysis of kinetic parameters used in calculations for "ITAMs" model. The variation of kinetic parameters for every chemical reaction was in the following parameter range: 0.001, 0.01, 0.1, 0.5, 1.0, 3.0, 5.0 s^{-1}.

(A) Sensitivity analysis for varying k_{cat} rate for production of singly phosphorylated N-terminal ITAMs ([Lck(A, Nsite):ITAM(N_0,C_0)] → Lck(A) + ITAM(N_p,C_0) reaction). For ZAP-70 null / ZAP-70 reconstituted SILAC ratio (top panel figures): at low rates ITAM phosphorylation asymmetry is not reproduced; at low rates ZAP-70 null / ZAP-70 reconstituted ratio for N-terminal ITAMs is lower than ratio for C-terminal ITAMs, since k_{cat} for phosphorylation of C-terminal ITAMs is higher. For ZAP-70^{AS}+Inhibitor / ZAP-70^{AS} SILAC ratio (bottom panel figures): there is no qualitative change.

(B) Sensitivity analysis for varying k_{cat} rate for production of doubly phosphorylated ITAMs from singly phosphorylated N-terminal ITAMs ([Lck(A):ITAM(N_p,C_0)] → Lck(A) + ITAM(N_p,C_p) reaction). For ZAP-70 null / ZAP-70 reconstituted SILAC ratio (top panel figures): at low rates ITAM phosphorylation asymmetry is not reproduced; at low rates ZAP-70 null / ZAP-70 reconstituted ratio for N-terminal ITAMs is greater than ratio for C-terminal ITAMs. For ZAP-70^{AS}+Inhibitor / ZAP-70^{AS} SILAC ratio (bottom panel figures): there is no qualitative change.

(C) Sensitivity analysis for varying k_{on} rate of ZAP-70 binding to singly phosphorylated N-terminal ITAMs (ITAM(N_p,C_0) + Z → [ITAM(N_p,C_0):Z] reaction). For ZAP-70 null / ZAP-70 reconstituted SILAC ratio (top panel figures): at low rates there is no qualitative change; at high rates ZAP-70 protects singly phosphorylated N-terminal ITAMs from dephosphorylation by phosphatases, causing decreased phosphorylation of C-terminal ITAMs in ZAP-70 reconstituted cells. For ZAP-70^{AS}+Inhibitor / ZAP-70^{AS} SILAC ratio (bottom panel figures): there is no qualitative change.

(D) Sensitivity analysis for varying k_{on} rate of ZAP-70 binding to singly phosphorylated C-terminal ITAMs (ITAM(N_0,C_p) + Z → [ITAM(N_0,C_p):Z] reaction). For ZAP-70 null / ZAP-70 reconstituted SILAC ratio (top panel figures): at low rates there is no qualitative change; at high rates ZAP-70 protects singly phosphorylated C-terminal ITAMs from dephosphorylation by phosphatases, causing decreased phosphorylation of N-terminal ITAMs in ZAP-70 reconstituted cells. For ZAP-70^{AS}+Inhibitor / ZAP-70^{AS} SILAC ratio (bottom panel figures): there is no qualitative change.

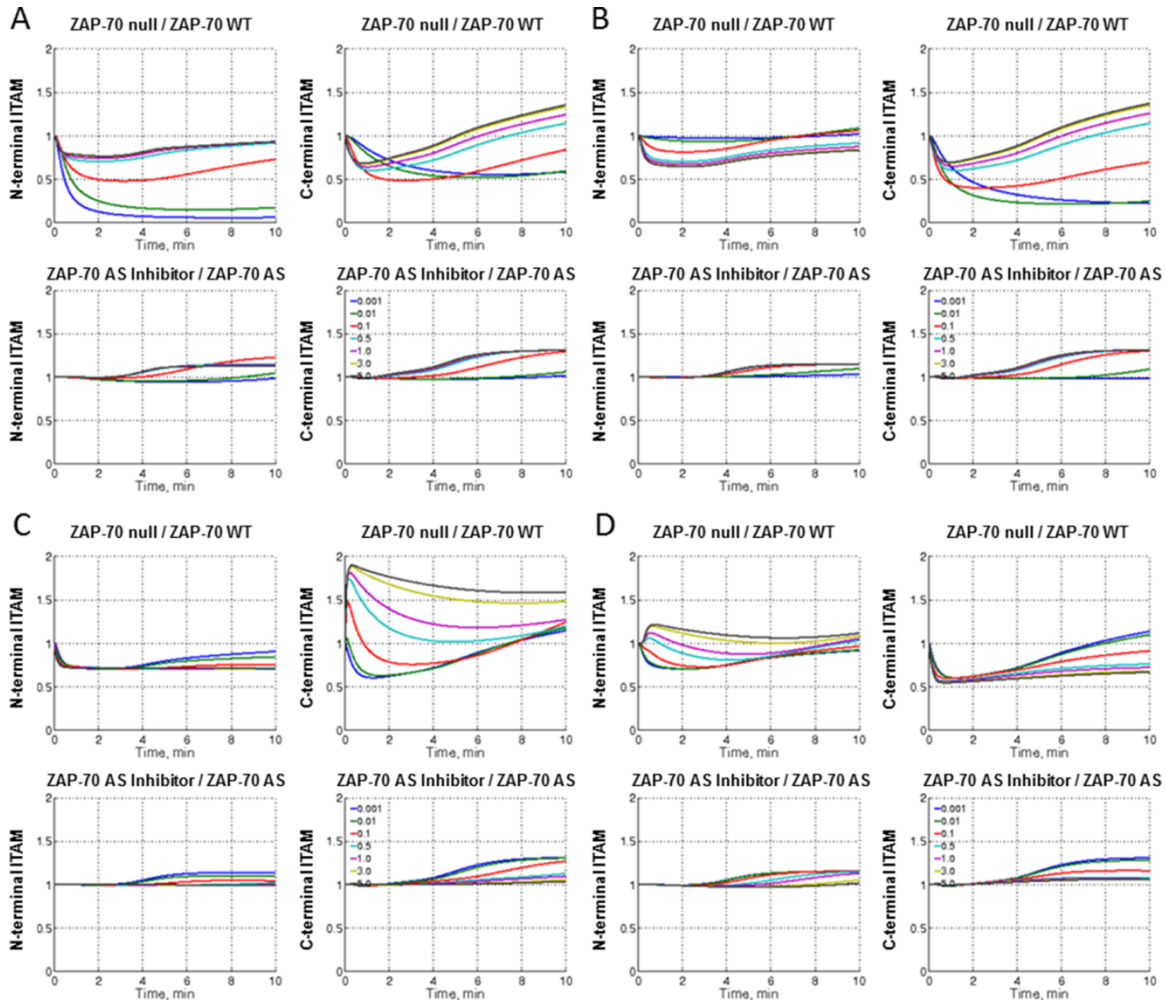

Table S11. Sensitivity analysis of concentrations of signaling molecules used in calculations for ZAP-70 allosteric model. The variation of number of molecules for every species was in the following parameter range: 100, 500, 1000, 1500, 2000 molecules.

Species*	Valid Parameter Range (no. of molecules)	Result
Lck(A)	all range	no qualitative change
ITAM(N_0,C_0)	all range	no qualitative change
P	all range	no qualitative change
Z	all range	no qualitative change
P_z	all range	no qualitative change

* Lck(A) is active Lck; ITAM(N_0,C_0) is unphosphorylated ITAMs; P is phosphatases dephosphorylating singly and doubly phosphorylated ITAMs; Z is ZAP-70; P_z is phosphatases dephosphorylating basal and active ZAP-70.

Table S12. Sensitivity analysis of kinetic parameters used in calculations for ZAP-70 allosteric model. The variation of kinetic parameters for every chemical reaction was in the following parameter range: 0.001, 0.01, 0.1, 0.5, 1.0, 3.0, 5.0 s^{-1}. Active Lck is denoted by Lck(A). ITAM(N_0,C_0), ITAM(N_p,C_0), ITAM(N_0,C_p) and ITAM(N_p,C_p) molecules denote unphosphorylated ITAMs, the singly phosphorylated tyrosine residue of N-terminal or C-terminal of ITAMs, and doubly phosphorylated ITAMs, correspondingly. ZAP-70 molecules exist in three states: ZAP-70 inactive, ZAP-70 basal and ZAP-70 fully active, which are labeled by Z, Z(B) and Z(A), respectively.

Reactions	**Valid Parameter Range (k_{on} $molec^{-1}s^{-1}$; k_{off}, k_{cat} s^{-1})**	**Result**
Lck(A) + ITAM(N_0,C_0) ↔ [Lck(A,Nsite):ITAM(N_0,C_0)]	k_{on}: all range k_{off}: all range	k_{on}: no qualitative change k_{off}: no qualitative change; at high rates the C-terminal ZAP-70 null / ZAP-70 reconstituted SILAC ratio is greater than N-terminal one, because Lck(A) unbinds faster from ITAMs prior its subsequent catalysis
[Lck(A,Nsite):ITAM(N_0,C_0)] → Lck(A) + ITAM(N_p,C_0)	all range	no qualitative change; at high rates the N-terminal ZAP-70 null / ZAP-70 reconstituted SILAC ratio is greater than C-terminal one (shown in Fig. S9A)
Lck(A) + ITAM(N_0,C_0) ↔ [Lck(A,Csite):ITAM(N_0,C_0)]	k_{on}: all range k_{off}: all range	k_{on}: no qualitative change k_{off}: no qualitative change; at high rates the N-terminal ZAP-70 null / ZAP-70 reconstituted SILAC ratio is greater than C-terminal one, because Lck(A) unbinds faster from ITAMs prior its subsequent catalysis
[Lck(A,Csite):ITAM(N_0,C_0)] → Lck(A) + ITAM(N_0,C_p)	all range	no qualitative change; at high rates the C-terminal ZAP-70 null / ZAP-70 reconstituted SILAC ratio is greater than N-terminal one (shown in Fig. S9B)
ITAM(N_p,C_0) + P ↔ [ITAM(N_p,C_0):P]	k_{on}: all range k_{off}: all range	k_{on}: no qualitative change k_{off}: no qualitative change; at high rates the N-terminal ZAP-70 null / ZAP-70 reconstituted SILAC ratio is greater than C-terminal one

$[ITAM(N_p,C_0):P] \rightarrow ITAM(N_0,C_0) + P$	all range	no qualitative change; at high rates the C-terminal ZAP-70 null / ZAP-70 reconstituted SILAC ratio is greater than N-terminal one (shown in Fig. S9C)
$ITAM(N_0,C_p) + P \leftrightarrow [ITAM(N_0,C_p):P]$	k_{on}: all range k_{off}: all range	k_{on}: no qualitative change k_{off}: no qualitative change; at high rates the C-terminal ZAP-70 null / ZAP-70 reconstituted SILAC ratio is greater than N-terminal one
$[ITAM(N_0,C_p):P] \rightarrow ITAM(N_0,C_0) + P$	all range	no qualitative change; at high rates the N-terminal ZAP-70 null / ZAP-70 reconstituted SILAC ratio is greater than C-terminal one (shown in Fig. S9D)
$Lck(A) + ITAM(N_p,C_0) \leftrightarrow [Lck(A):ITAM(N_p,C_0)]$	k_{on}: all range k_{off}: all range	k_{on}: no qualitative change k_{off}: no qualitative change
$[Lck(A):ITAM(N_p,C_0)] \rightarrow Lck(A) + ITAM(N_p,C_p)$	all range	no qualitative change
$Lck(A) + ITAM(N_0,C_p) \leftrightarrow [Lck(A):ITAM(N_0,C_p)]$	k_{on}: all range k_{off}: all range	k_{on}: no qualitative change k_{off}: no qualitative change
$[Lck(A):ITAM(N_0,C_p)] \rightarrow Lck(A) + ITAM(N_p,C_p)$	all range	no qualitative change
$ITAM(N_p,C_p) + P \leftrightarrow [ITAM(N_p,C_p):P(Nsite)]$	k_{on}: all range k_{off}: all range	k_{on}: no qualitative change k_{off}: no qualitative change
$[ITAM(N_p,C_p):P(Nsite)] \rightarrow ITAM(N_0,C_p) + P$	all range	no qualitative change
$ITAM(N_p,C_p) + P \leftrightarrow [ITAM(N_p,C_p):P(Csite)]$	k_{on}: all range k_{off}: all range	k_{on}: no qualitative change k_{off}: no qualitative change
$[ITAM(N_p,C_p):P(Csite)] \rightarrow ITAM(N_p,C_0) + P$	all range	no qualitative change
$ITAM(N_p,C_0) + Z \leftrightarrow [ITAM(N_p,C_0):Z]$	k_{on}: less than 0.01 k_{off}: all range	k_{on}: at low rates – no qualitative change; at high rates – observed artifact: the ZAP-70 protects the singly phosphorylated N-terminal ITAMs from dephosphorylation by phosphatases, causing the increased production of the phosphorylated C-terminal ITAMs (shown in Fig. S10A) k_{off}: no qualitative change
$ITAM(N_0,C_p) + Z \leftrightarrow [ITAM(N_0,C_p):Z]$	k_{on}: less than 0.01 k_{off}: all range	k_{on}: at low rates – no qualitative change; at high rates – observed artifact: the ZAP-70 protects the singly phosphorylated C-terminal ITAMs from dephosphorylation by phosphatases, causing the increased production of the phosphorylated N-terminal ITAMs (shown in Fig. S10B) k_{off}: no qualitative change

$ITAM(N_p,C_p) + Z \leftrightarrow [ITAM(N_p,C_p):Z]$	k_{on}: all range k_{off}: all range	k_{on}: no qualitative change; at high rates the ZAP-70 null / ZAP-70 reconstituted SILAC ratio decreases for N- and C- terminals of ITAMs due to the ZAP-70 protective function (shown in Fig. S10C) k_{off}: no qualitative change If K_D of ZAP-70^{AS}+Inhibitor cells equals to K_D of ZAP-70^{AS} cells, the experimental data for ZAP-70^{AS}+Inhibitor / ZAP-70^{AS} SILAC ratio are not reproduced (shown in Fig. S10C)
$[ITAM(N_p,C_p):Z] + Lck(A) \leftrightarrow [ITAM(N_p,C_p):Z:Lck(A)]$	k_{on}: all range k_{off}: all range	k_{on}: no qualitative change k_{off}: no qualitative change
$[ITAM(N_p,C_p):Z:Lck(A)] \rightarrow [ITAM(N_p,C_p):Z(B)]+Lck(A)$	all range	no qualitative change
$[ITAM(N_p,C_p):Z(B)] + P_z \leftrightarrow [ITAM(N_p,C_p):Z(B):P_z]$	k_{on}: all range k_{off}: all range	k_{on}: no qualitative change k_{off}: no qualitative change
$[ITAM(N_p,C_p):Z(B):P_z] \rightarrow [ITAM(N_p,C_p):Z] + P_z$	all range	no qualitative change
$[ITAM(N_p,C_p):Z(B)] \leftrightarrow [ITAM(N_p,C_p):Z(B, open)]$	k_{on}: all range k_{off}: all range	k_{on}: no qualitative change k_{off}: no qualitative change
$[ITAM(N_p,C_p):Z(B, open)] + Lck(A) \leftrightarrow$ $[ITAM(N_p,C_p):Z(B, open):Lck(A, SH2)]$	k_{on}: all range k_{off}: all range	k_{on}: no qualitative change k_{off}: no qualitative change
$[ITAM(N_p,C_p):Z(B, open):Lck(A, SH2)] \rightarrow$ $[ITAM(N_p,C_p):Z(A)] + Lck(A)$	all range	no qualitative change
$[ITAM(N_p,C_p):Z(A)] + P_z \leftrightarrow [ITAM(N_p,C_p):Z(A):P_z]$	k_{on}: all range k_{off}: all range	k_{on}: no qualitative change k_{off}: no qualitative change
$[ITAM(N_p,C_p):Z(A):P_z] \rightarrow$ $[ITAM(N_p,C_p):Z(B, open)] + P_z$	all range	no qualitative change
$[ITAM(N_p,C_p):Z(B, open)] + P_z \leftrightarrow$ $[ITAM(N_p,C_p):Z(B, open):P_z]$	k_{on}: all range k_{off}: all range	k_{on}: no qualitative change k_{off}: no qualitative change
$[ITAM(N_p,C_p):Z(B, open):P_z] \rightarrow$ $[ITAM(N_p,C_p):Z] + P_z$	all range	no qualitative change

Fig. S9. Sensitivity analysis of kinetic parameters used in calculations for ZAP-70 allosteric model. The variation of kinetic parameters for every chemical reaction was in the following parameter range: 0.001, 0.01, 0.1, 0.5, 1.0, 3.0, 5.0 s^{-1}.

(A) Sensitivity analysis for varying k_{cat} rate for production of singly phosphorylated N-terminal ITAMs ($[Lck(A, Nsite):ITAM(N_0,C_0)] \rightarrow Lck(A) + ITAM(N_p,C_0)$ reaction). For ZAP-70 null / ZAP-70 reconstituted SILAC ratio (top panel figures): at low rates there is no qualitative change; at high rates the N-terminal ZAP-70 null / ZAP-70 reconstituted SILAC ratio is greater than C-terminal one. For ZAP-70^{AS}+Inhibitor / ZAP-70^{AS} SILAC ratio (bottom panel figures): there is no qualitative change.

(B) Sensitivity analysis for varying k_{cat} rate for production of singly phosphorylated C-terminal ITAMs ($[Lck(A, Csite):ITAM(N_0,C_0)] \rightarrow Lck(A) + ITAM(N_0,C_p)$ reaction). For ZAP-70 null /

ZAP-70 reconstituted SILAC ratio (top panel figures): at low rates there is no qualitative change; at high rates the C-terminal ZAP-70 null / ZAP-70 reconstituted SILAC ratio is greater than N-terminal one. For ZAP-70^{AS}+Inhibitor / ZAP-70^{AS} SILAC ratio (bottom panel figures): there is no qualitative change.

(C) Sensitivity analysis for varying k_{cat} rate for dephosphorylation of singly phosphorylated N-terminal ITAMs to its unphosphorylated form by phosphatases ([ITAM(N_p,C_0):P] → ITAM(N_0,C_0) + P reaction). For ZAP-70 null / ZAP-70 reconstituted SILAC ratio (top panel figures): at low rates there is no qualitative change; at high rates the C-terminal ZAP-70 null / ZAP-70 reconstituted SILAC ratio is greater than N-terminal one. For ZAP-70^{AS}+Inhibitor / ZAP-70^{AS} SILAC ratio (bottom panel figures): there is no qualitative change.

(D) Sensitivity analysis for varying k_{cat} rate for dephosphorylation of singly phosphorylated C-terminal ITAMs to its unphosphorylated form by phosphatases ([ITAM(N_0,C_p):P] → ITAM(N_0,C_0) + P reaction). For ZAP-70 null / ZAP-70 reconstituted SILAC ratio (top panel figures): at low rates there is no qualitative change; at high rates the N-terminal ZAP-70 null / ZAP-70 reconstituted SILAC ratio is greater than C-terminal one. For ZAP-70^{AS}+Inhibitor / ZAP-70^{AS} SILAC ratio (bottom panel figures): there is no qualitative change.

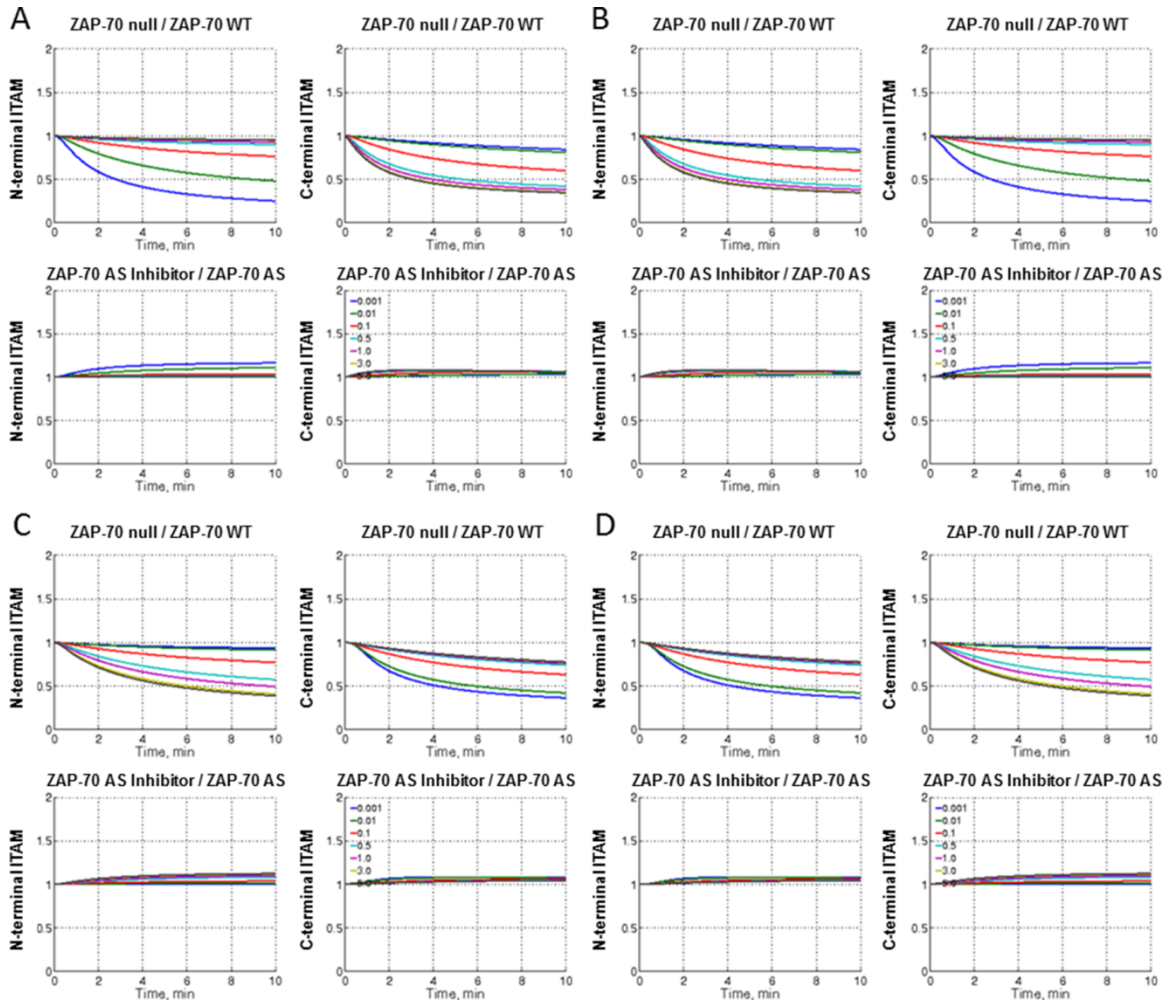

Fig. S10. Sensitivity analysis of varying kinetic parameters used in calculations for ZAP-70 allosteric model. The variation of kinetic parameters for every chemical reaction was in the following parameter range: 0.001, 0.01, 0.1, 0.5, 1.0, 3.0, 5.0 s^{-1}.

(A) Sensitivity analysis for varying k_{on} rate of ZAP-70 binding to singly phosphorylated N-terminal ITAMs ($ITAM(N_p,C_0) + Z \rightarrow [ITAM(N_p,C_0):Z]$ reaction). For ZAP-70 null / ZAP-70 reconstituted SILAC ratio (top panel figures): at low rates there is no qualitative change; at high rates ZAP-70 protects singly phosphorylated N-terminal ITAMs from dephosphorylation by phosphatases, causing an increased production of phosphorylated C-terminal ITAMs. For ZAP-70^{AS}+Inhibitor / ZAP-70^{AS} SILAC ratio (bottom panel figures): there is no qualitative change.

(B) Sensitivity analysis for varying k_{on} rate of ZAP-70 binding to the singly phosphorylated C-terminal ITAMs ($ITAM(N_0,C_p) + Z \rightarrow [ITAM(N_0,C_p):Z]$ reaction). For ZAP-70 null / ZAP-70 reconstituted SILAC ratio (top panel figures): at low rates there is no qualitative change; at high rates ZAP-70 protects singly phosphorylated C-terminal ITAMs from dephosphorylation by

phosphatases, causing an increased production of phosphorylated N-terminal ITAMs. For ZAP-70^{AS}+Inhibitor / ZAP-70^{AS} SILAC ratio (bottom panel figures): there is no qualitative change.

(C) Sensitivity analysis for varying k_{on} rate of ZAP-70 binding to doubly phosphorylated ITAMs (ITAM(N_p,C_p) + Z → [ITAM(N_p,C_p):Z] reaction). For ZAP-70 null / ZAP-70 reconstituted SILAC ratio (top panel figures): at low rates there is no qualitative change; at high rates ZAP-70 protects doubly phosphorylated ITAMs from dephosphorylation by phosphatases. If K_D of ZAP-70^{AS}+Inhibitor equals to K_D of ZAP-70^{AS}, the experimental data for ZAP-70^{AS}+Inhibitor / ZAP-70^{AS} SILAC ratio are not reproduced (bottom panel figures).

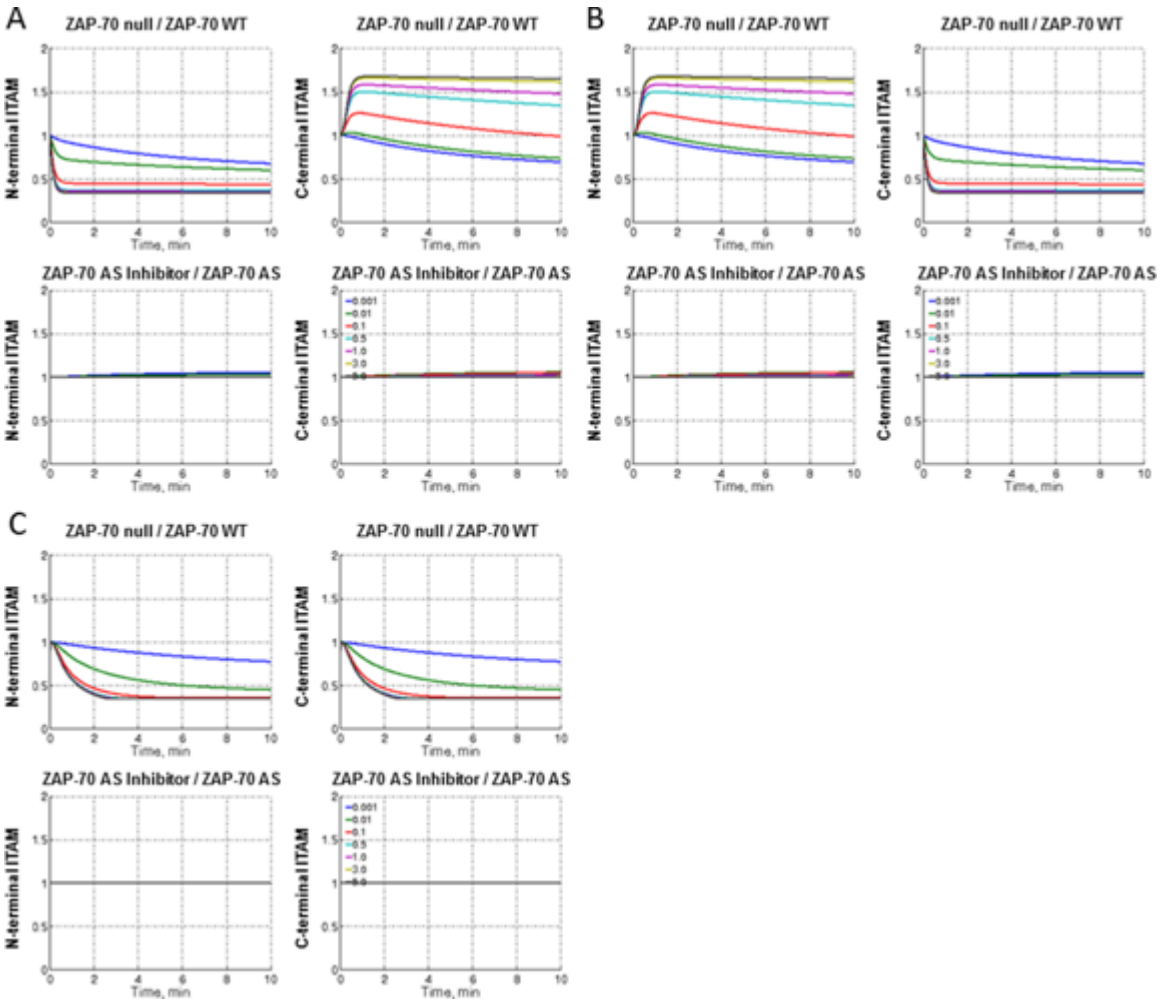

References

1. V. Nguyen *et al.*, A New Approach for Quantitative Phosphoproteomic Dissection of Signaling Pathways Applied to T Cell Receptor Activation. *Mol. Cell. Proteomics*. **8**, 2418–2431 (2009).

2. J. Rappsilber, Y. Ishihama, M. Mann, Stop and Go Extraction Tips for Matrix-Assisted Laser Desorption/Ionization, Nanoelectrospray, and LC/MS Sample Pretreatment in Proteomics. *Anal. Chem.* **75**, 663–670 (2003).

3. K. Yu, A. R. Salomon, PeptideDepot: Flexible relational database for visual analysis of quantitative proteomic data and integration of existing protein information. *PROTEOMICS*. **9**, 5350–5358 (2009).

4. K. Yu, A. R. Salomon, HTAPP: High-throughput autonomous proteomic pipeline. *PROTEOMICS*. **10**, 2113–2122 (2010).

5. S. B. Ficarro *et al.*, Automated immobilized metal affinity chromatography/nano-liquid chromatography/electrospray ionization mass spectrometry platform for profiling protein phosphorylation sites. *Rapid Commun. Mass Spectrom. RCM*. **19**, 57–71 (2005).

6. D. N. Perkins, D. J. Pappin, D. M. Creasy, J. S. Cottrell, Probability-based protein identification by searching sequence databases using mass spectrometry data. *Electrophoresis*. **20**, 3551–3567 (1999).

7. K. Yu *et al.*, Integrated platform for manual and high-throughput statistical validation of tandem mass spectra. *PROTEOMICS*. **9**, 3115–3125 (2009).

8. J. E. Elias, S. P. Gygi, Target-decoy search strategy for increased confidence in large-scale protein identifications by mass spectrometry. *Nat. Methods*. **4**, 207–214 (2007).

9. S. A. Beausoleil, J. Villén, S. A. Gerber, J. Rush, S. P. Gygi, A probability-based approach for high-throughput protein phosphorylation analysis and site localization. *Nat. Biotechnol.* **24**, 1285–1292 (2006).

10. J. D. Storey, The positive false discovery rate: a Bayesian interpretation and the q -value. *Ann. Stat.* **31**, 2013–2035 (2003).

11. J. D. Storey, R. Tibshirani, Statistical significance for genomewide studies. *Proc. Natl. Acad. Sci.* **100**, 9440–9445 (2003).

12. H. Edelhoch, Spectroscopic determination of tryptophan and tyrosine in proteins. *Biochemistry (Mosc.)*. **6**, 1948–1954 (1967).

13. N. J. Anthis, G. M. Clore, Sequence-specific determination of protein and peptide concentrations by absorbance at 205 nm. *Protein Sci. Publ. Protein Soc.* **22**, 851–858 (2013).

14. M. R. Clark, S. A. Johnson, J. C. Cambier, Analysis of Ig-alpha-tyrosine kinase interaction reveals two levels of binding specificity and tyrosine phosphorylated Ig-alpha stimulation of Fyn activity. *EMBO J.* **13**, 1911–1919 (1994).

15. S. M. Abel, J. P. Roose, J. T. Groves, A. Weiss, A. K. Chakraborty, The Membrane Environment Can Promote or Suppress Bistability in Cell Signaling Networks. *J. Phys. Chem. B*. **116**, 3630–3640 (2012).

16. E. Hui, R. D. Vale, In vitro membrane reconstitution of the T-cell receptor proximal signaling network. *Nat. Struct. Mol. Biol.* **21**, 133–142 (2014).

17. G. I. Bell, Models for the specific adhesion of cells to cells. *Science*. **200**, 618–627 (1978).

18. C. C. Govern, M. K. Paczosa, A. K. Chakraborty, E. S. Huseby, Fast on-rates allow short dwell time ligands to activate T cells. *Proc. Natl. Acad. Sci. U. S. A.* **107**, 8724–8729 (2010).

19. M. E. Labadia, R. H. Ingraham, J. Schembri-King, M. M. Morelock, S. Jakes, Binding affinities of the SH2 domains of ZAP-70, p56lck and Shc to the zeta chain ITAMs of the T-cell receptor determined by surface plasmon resonance. *J. Leukoc. Biol.* **59**, 740–746 (1996).

20. S. Deindl, T. A. Kadlecek, X. Cao, J. Kuriyan, A. Weiss, Stability of an autoinhibitory interface in the structure of the tyrosine kinase ZAP-70 impacts T cell receptor response. *Proc. Natl. Acad. Sci.* **106**, 20699–20704 (2009).

21. H. Mukhopadhyay, S.-P. Cordoba, P. K. Maini, P. A. van der Merwe, O. Dushek, Systems Model of T Cell Receptor Proximal Signaling Reveals Emergent Ultrasensitivity. *PLoS Comput. Biol.* **9**, e1003004 (2013).

22. H. R. Housden *et al.*, Investigation of the kinetics and order of tyrosine phosphorylation in the T-cell receptor zeta chain by the protein tyrosine kinase Lck. *Eur. J. Biochem.* **270**, 2369–2376 (2003).

23. M. N. Artyomov, M. Lis, S. Devadas, M. M. Davis, A. K. Chakraborty, CD4 and CD8 binding to MHC molecules primarily acts to enhance Lck delivery. *Proc. Natl. Acad. Sci.* **107**, 16916–16921 (2010).

24. S. Mukherjee *et al.*, Monovalent and Multivalent Ligation of the B Cell Receptor Exhibit Differential Dependence upon Syk and Src Family Kinases. *Sci. Signal.* **6**, ra1–ra1 (2013).

25. A. C. Chan *et al.*, Activation of ZAP-70 kinase activity by phosphorylation of tyrosine 493 is required for lymphocyte antigen receptor function. *EMBO J.* **14**, 2499–2508 (1995).

26. E. Tsang *et al.*, Molecular Mechanism of the Syk Activation Switch. *J. Biol. Chem.* **283**, 32650–32659 (2008).